Copernicus Climate Change

Integration of Climate Data in the SAVi Energy Model

C3S_428h_IISD-EU: Sustainable Asset Valuation (SAVi): Demonstrating the Business Case for Climate-Resilient and Sustainable Infrastructure

Issued by: IISD-EU / Oshani Perera

Date: September 2020

Ref:

C3S_428h_IISD-EU_D428h.1.1 _202006_Integration of climate data in the SAVi model_v2

Official reference number service contract:

2019/C3S_428h_IISD-EU/SC1

Contributors

International Institute for Sustainable Development
Bechauf, Ronja
Casier, Liesbeth
Lago, Sergio
Perera, Oshani
Perrette, Mahé
Uzsoki, David
Wuennenberg, Laurin

KnowlEdge Srl
Bassi, Andrea M.
Pallaske, Georg

Table of Contents

1 About This Report

This report outlines the integration of authoritative Copernicus Climate Data from the Climate Data Store (CDS) into the Sustainable Asset Valuation (SAVi) tool. It describes how several climate indicators obtained from the CDS were integrated into the SAVi Energy model and how the analysis performed by SAVi has improved as a result. In light of this integration, IISD is able to generate sophisticated SAVi-derived analyses on the costs of climate-related risks and climate-related externalities.

The integration of Copernicus Climate Data into other SAVi models for roads, irrigation, wastewater treatment infrastructure, buildings, and nature-based infrastructure can be found here.

This document presents:

- A summary of the literature review on the impact of climate variables on energy (power generation) infrastructure, including equations that link climate variables to the economic performance of various power generation technologies as well as power grid efficiency: wind technology, wave technology, solar technology, hydropower, gas power, coal power, nuclear power, geothermal power, and power grid.
- How the above information was used to select relevant indicators from the Copernicus database.
- How outputs of the CDS datasets are integrated into the SAVi System Dynamics (SD) Energy model.
- How simulation results can be affected by this new and improved set of indicators.

The different sections of this document are organized as follows.

Literature Review

The literature review is organized per power generation technology and contains the following subsections for each climate variable discussed per technology:

- Subsection 1: An overview of climate impacts on the asset (e.g., how air temperature affects solar technology).
- Subsection 2: A presentation of research results found in papers/reports that provide case studies on the range of impacts estimated or observed (e.g., across countries).
- Subsection 3: A description of the methodology found in the literature for the calculation of climate impacts on the infrastructure asset.
- Subsection 4: A selection of CDS datasets required by the equations.

Integration of the Literature Review With the CDS Dataset

This section summarizes information on what datasets are being used from the Copernicus database and what additional processing was applied before integrating these into the SAVi Energy model. We first review the equations to determine their usefulness for the various power generation technologies of the SAVi Energy model. We then assess what data requirements for each of the equations are available in the Copernicus database and create indicators for climate variables that are relevant for the equations selected. Finally, in certain cases, we create indicators in the CDS Toolbox for first-order impacts on power generation infrastructure. Second- and third-order impacts will be estimated with SAVi, making use of additional equations included in the SD model.

Integration of Climate Indicators Into the SAVi Energy Model

This section explains how the CDS indicators are used in the SAVi SD model for Energy (power generation) infrastructure. This includes the identification of specific indicators of performance for each asset impacted by climate indicators (e.g., efficiency and cost).

Behavioural Impacts Resulting From the Integration of Climate Variables

This section discusses how climate variables affect asset performance in the SD model, providing early insights as to how the results of the SAVi analysis may change when equipping the model with more and better refined climate indicators (e.g., with the cost of energy infrastructure being higher due to increased maintenance, the economic viability of the infrastructure asset, expressed as the Internal Rate of Return [IRR], will be lower than expected).

Simulation Results

The final section of this paper presents the equations used and quantitative results emerging from the inclusion of climate indicators in the SAVi Energy model under various climate scenarios. This is the end product of the enhanced SAVi model, which is used to inform policy and investment decisions for infrastructure. Table 1 provides an overview of climate drivers, impacts, and relevant SAVi output indicators for power generation infrastructure.

The CDS datasets are accessed via the CDS application programming interface (API), and additional processing and packaging for use in SAVi are done offline. Technical information about the offline code is found in Annex I. We also selected a subset of the most-used indicators and created an app in the CDS Toolbox with interactive visualization for demonstration purposes.

Table 1 Overview of variables and impacts implemented in the SAVi Energy model

SAVi module	Implemented impact	Main climate drivers	Affected output indicators
Energy (power generation)	Impact on load factor	• Coal: Temperature • Gas: Temperature • Nuclear: Temperature • Biomass: Temperature • Hydro: Precipitation • Wind: Wind speed • Solar: Temperature	• Electricity generation • Revenues from electricity generation • Fuel expenditure • Energy-related emissions (for fossil fuel generators) • Social cost of carbon • Cost of air pollution
	Impact on thermal efficiency	• All thermal generators: Temperature	• Fuel use • Fuel expenditure • Fuel use • Fuel-related emissions • Social cost of carbon
	Impact on grid efficiency	• Temperature	• Revenues from electricity sales

2 Power generation infrastructure

2.1 Literature review

2.1.1 Wind technology

2.1.1.1 Wind Speed

Wind turbines convert wind kinetic energy into electricity, or electric energy. It results that changes in mean wind speed have an impact on wind power generation (Harrison & Wallace, 2005).
There are many types of wind turbines, which can be grouped into vertical axis and horizontal axis. This review covers only turbines with horizontal axis.
The components of a wind turbine are the rotor, the generator, and the surrounding structure.

- **Climate impact**

Wind power generation is affected by wind speed. If there is no or too little wind, turbines cannot produce electricity. On the contrary, when the wind speed is too strong, efficiency is lost because turbines have a cut-out limit and stop generating electricity.

- **Summary of results**

In Scotland, Harrison and Wallace (2005) estimate that the range of variation of change in wind speed (m/s) [-20; -10; +10; +20] impact on turbine output from base case is of [-26,06%; - 11,52%; +8,37%; +13,66%]. For Davy et al. (2018) , from RCP 4.5 and RCP 8.5 for CIMP5, the prevision of the impact of change in wind speed to extractable power is under 10% for both scenarios.

- **Results**

The relationship between wind speed and power generation output has been documented by Manwell et al. (2010; 2002). Many other studies present similar information for other types of wind turbines (considering technology, size and location of installation). Harrison and Wallace (2005) focused on offshore turbines located in Western Scotland. Figure 1 shows power generation in relation to changes in wind speed.

Figure 1 Wind turbine performance altered by wind speed

Wind turbine performance with base case and uniformly altered wind speed

Measure	Base case	Annual mean wind speed change (%)			
		−20	−10	+10	+20
Mean turbine output (kW)	1493	1104	1321	1618	1697
Production (GWh/year)	13.08	9.67	11.57	14.17	14.85

Davy et al. (2018) focused on extractable power energy in the region of the Black Sea for a 120 m hub-height turbine, 7.6 MW capacity, Enercon E-126 turbine). He showed that under RCP 4.5 and RCP 8.5 scenario, on average, the projected changes to the EWP (Extractable Wind Power) in all cases are small (< 10% of the historical EWP (1979-2004)) and there is a 15–20% difference in the EWP and WPD (Wind Power Density) over the different regions of the Black Sea.

- **Methodology**

Method 1 (Harrison & Wallace, 2005)

1. Wind Energy

Power in wind varies with the cube of the wind speed U (m/s) such as:

$$P = \frac{1}{2}\rho U^3$$

Where P is the power per unit area (W/m2) and “rho” is the air density. Turbine Output is defined by production curves, which specify output over the wind speed range between the cut-in and cut-out speeds. When combined with the wind speed information, production and, with appropriate data, the economic performance can be estimated.

2. Wind speed distribution

A range of models have been used to describe the wind resource including the well-known Weibull distribution. A special case of this, the Rayleigh distribution, is commonly used and is defined solely by the mean wind speed U (mean):

$$p(U) = \frac{\pi}{2}\left(\frac{U}{\bar{U}^2}\right)\exp\left[-\frac{\pi}{4}\left(\frac{U}{\bar{U}}\right)^2\right]$$

Here p (U) is the probability of occurrence of wind speed U and when modelled incrementally, it gives the probability and, for a given period, the duration of time (in hours) for which each wind speed increment is experienced. The use of the appropriate wind turbine output at each increment and summation across all increments provides an estimate of energy production in the period.

Particular application: *West coast of Scotland* (Harrison & Wallace, 2005)

The wind speed was defined in 0.25 m/s increments (up to 30 m/s) with the probability of occurrence and duration calculated from wind speed distribution function.
In order to maintain simplicity, the mean annual wind speed (at 19.5 m) was estimated at 10 m/s (base case). The turbine chosen for the analysis is the 3 MW Vestas V90. (Young & Holland, 1996)
The corrected mean wind speed at hub height was found to be just over 11 m/s using the power law profile:

$$U_{65} = U_{19.5}\frac{\ln(h_{65}/z_0)}{\ln(h_{19.5}/z_0)}$$

Where h65 and h19.5 are the hub and reference heights while z0 is the roughness length of the water surface which is generally very low. The turbine power curve follows the traditional shape with cut-in at 4 m/s, cut-out at 25 m/s and rated output at 15 m/s

Considerations for integration in the CDS toolbox

Units**:** Wind speed = m/s, air density = kg m^{-3}
ERA5 monthly averaged and hourly data on single levels from 1979 to present Wind speed, Air density

- CORDEX regional climate model data on single levels for Europe (Wind speed)
- CMIP5 monthly data on single levels (Wind speed)

Method 2 (Davy, Gnatiuk, Pettersson, & Bobylev, 2018)

Intensity and variability of near surface winds and roughness impacts wind energy production.

"*While it is common to use simple power-law approximations to extrapolate wind speeds to turbine hub-heights, in this work we developed a roughness-length dependency in our calculation of wind speeds based on established boundary-layer profiles for winds***"**

1. Wind Speed

$$W_z = \frac{u_*}{k} ln \frac{z}{z_0}$$

Where W_z is the wind speed at height z; k is the von Karman constant, taken to be 0.4; z_0 is the roughness length; and u_* is the friction velocity.

2. The friction velocity

U_* is calculated from the surface wind stress (τ) and the air density (ρ):

$$u_* = \sqrt{\tau/\rho} \qquad (2)$$

$$\text{where } \tau = \sqrt{\tau_U^2 + \tau_V^2}, \text{ and we take } \rho = p_s/RT_s, \text{ with } R = 287.06 \text{ J kg}^{-1} \text{ K}^{-1}.$$

With T_s being surface air temperature, P_s being surface pressure and T_u and T_v being surface wind stress.

For (1) and (2) we have to calculate the friction velocity from the available data using (2), and then use the 10 m wind speeds to calculate the roughness length using Wind speed eq. We enforced a lower limit on the roughness length, based on values found over calm water, such that z ≥ 0.0002m. The derived friction velocity and roughness length were then substituted back into wind speed eq. to obtain the wind speed at a height of 120 m above the surface–the turbine height.

Note that (1) includes an implicit assumption that the atmosphere is neutrally-stratified, and in principle a term accounting for the stability of the atmosphere should be included. However, this was not possible here given the limited availability of data.

As a result, when we use this formulation to estimate wind speeds at 120 m, we will tend to overestimate wind speeds in convective conditions and under-estimate wind speeds instably-stratified conditions.

3. Wind Power Density (WPD):

The power (P) per unit area (A), is defined from the air density (ρ) and the wind speed (W):

$$WPD = \frac{P}{A} = \frac{1}{2}\overline{\rho W^3}$$

Where W is wind speed at height of 120m and over-bar indicates an averaging over time. WPD sensitive to small-timescale variations in wind speed because of this cubed-dependence. Here constrained to use daily-mean wind speed data so WPD will be under-estimated. We used 3 hourly resolutions and compared by doing W^3 (3hr)/W^3 (daily) for each day.

Biggest difference seen in Mediterranean region with less than 20% difference over water although still geographical variations.

4. Extractable Wind Power (EWP)

A power-curve data from a typical 120 m hub-height wind turbine was used. The data is from the high capacity, 7.6 MW Enercon E-126 turbine (see Figure 2):

Figure 2 Normalized power curve

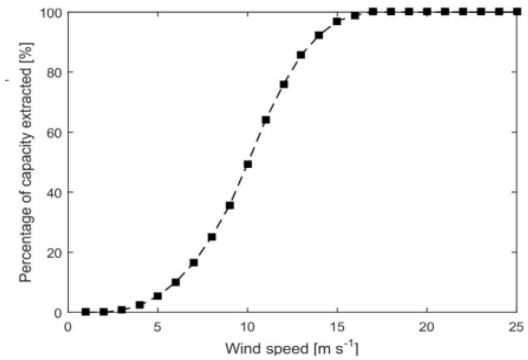

A spline interpolation was used to calculate the Wind Power produced at each time-step, which was then averaged over the period of interest to obtain the typical EWP for a given location (Davy, Gnatiuk, Pettersson, & Bobylev, 2018).

Considerations for integration in the CDS toolbox

- Input: ERA5, hourly data, 100m_u_component_of_wind and 100m_v_component_of_wind
- wind power density ½ rho U**3
- extractable wind power (look-up)

We select wind speed at 100 m from ERA5, on an hourly basis, as it represents more accurately the wind experienced by large turbines, unaffected by the boundary layer. For future projections, we use CMIP5, 10-m wind speed at daily resolution, which we scale to match ERA5 100-m during the period of overlap (2006 to 2019, which resulted in a scaling coefficient of 1.65).

- Two scenarios were used: RCP 4.5 and RCP 8.5 for CMIP5
- Units: Wind speed = m/s, Surface pressure = Pa, Surface air temperature = K, Roughness length = m, air density = kg m^{-3}, Surface wind stress =?
- Daily data are used in the article:
  - CORDEX regional climate model data on single levels for Europe (Wind speed)
  - CMIP5 daily and monthly data on single levels (Wind speed)
  - ERA5 hourly and monthly averaged data on single levels from 1979 to present (Wind speed, surface air temperature, air density)
  - ERA5-Land hourly and monthly averaged data from 1981 to present (Surface Pressure)

Method 3 (Manwell, McGowan, & Rogers, 2010)

Mass flow of air d*m*/d*t*, through a rotor disc of area A can be determined with an equation involving air density and air velocity:

$$\frac{dm}{dt} = \rho AU$$

The kinetic energy per unit time of the flow is then calculated:

$$P = \frac{1}{2}\frac{dm}{dt}U^2 = \frac{1}{2}\rho AU^3$$

Which we can transform to get the wind power per area *P/A*:

$$\frac{P}{A} = \frac{1}{2}\rho U^3$$

Note: conditions assumed here are sea-level, 15˚C and density of air of 1.225 kg/m^3. Power from wind is proportional to area swept by the rotor and wind power density is proportional to the cube of the wind velocity.

Considerations for integration in the CDS toolbox

ERA5 hourly and monthly averaged data on single levels from 1979 to present

Method 4 (Farkas, 2011)

P=1/2 ×the density of air ×the area swept out by the turbines × (wind speed) ^{3}

The most important variable is wind speed. The area swept out by the turbine is a constant and the density of air is generally taken as 1.225 kg/m^3, its value at sea level at 15 degrees Celsius.

Considerations for integration in the CDS toolbox

ERA5 hourly and monthly averaged data on single levels from 1979 to present

2.1.2 Wave Technology

Some of the kinetic (motional) energy in the wind is transformed into waves once the wind hits the ocean surface. Most of the energy comes from the rising and falling water level and requires exposure to the waves.
There are three main technologies that are Oscillating Water Column (OWC), Surface-following attenuator (Line Absorber) and Buoyancy Unit/Point Absorber. There might never be a dominant technology for harnessing this power because of the differences in potential wave energy sites throughout the world.

2.1.2.1 Wind Speed

- **Climate impact**

As ocean waves are predominantly the result of wind action, changes in wind patterns will ultimately alter wave regimes. Waves are created by the transfer of energy from wind flowing over water bodies. The energy transfer defines the size of waves and this is dependent on the strength and duration of the wind and the available fetch (Harrison & Wallace, 2005).

- **Summary of results**

Harrison and Wallace (2005) estimate that the range of impact of change in wind speed (m/s) [-20%; -10%; +10%; +20%] on wave energy production (GWh/year) from base case is of [-42,16%; -21,08%; +20,1%; +38,73%].

- **Results**

Harrison and Wallace (2005) estimated the impact of wind speed on wave power generation (Surface-following attenuator, see Figure 3). More details on the methodology are presented next.

Figure 3 Wave energy and changes in wind speed

Wave energy and device performance with base case and uniformly altered wind speed

Measure	Base case	Annual mean wind speed change (%)			
		−20	−10	+10	+20
Mean wave height, H_S (m)	2.70	1.73	2.19	3.27	3.88
Mean wave period, T_e (s)	6.25	5.00	5.63	6.88	7.50
Mean available wave power (kW/m)	83.7	27.5	49.5	134.4	205.6
Mean device power output (kW)	232.8	134.4	183.8	279.4	322.5
Production (GWh/year)	2.04	1.18	1.61	2.45	2.83
Load factor (%)	31.0	17.9	24.5	37.3	43.0

- **Methodology**

1. Wave energy (Evans & Antonio, 1986)

The power in the waves varies with the square of the wave height and linearly with wave period; and can be defined as follows:

$$P = 0.49 H_S T_e$$

Where P is power (kW/m of wave front), H_s is the significant wave height (m) and T_e the wave energy period (s). H_s and T_e are representative of the wide spectrum of waves of different heights,

periods and directions that make up real seas. Together they allow the specification of a range of "sea states" that have given probability of occurrence based on the joint coincidence of H_s and T_e.

H_s is defined as four times the root-mean-square (RMS) elevation of the sea surface (H_{rms}) and where m0 is the zero moment (or variance) of the wave spectrum.

$$H_S = 4H_{rms} = 4\sqrt{m_0}$$

T_e is defined as the Energy period which is one of several representative wave period measures in use although it is favored for wave energy approaches as it weights waves according to spectral energy content where m-1is the reciprocal of the first spectral moment (the mean frequency):

$$T_e = m_{-1}/m_0$$

2. Wind-wave Model (Pierson Jr & Moskowitz, 1964)

The relationship between wind and wave conditions can be defined using the classic Pierson–Moskowitz (PM) spectrum.
This describes fully developed (steady-state) wind-created seas that may occur when the wind has been blowing over a long period (6–18 h) and fetch (200–600 km). The spectrum is empirically derived and uses the wind speed, U_0 (at a height of 19.5 m above mean sea level) as the single parameter that defines the energy spectrum of wave energies:

$$S(\omega) = 0.0081 g^2 \omega^{-5}\, 0.25 \exp\left[-0.74\left(\frac{g}{U_0\omega}\right)^4\right]$$

Where S (u) is the spectral energy as a function of frequency, u (rads). Practical use is through determination of H_s and T_e through analysis of the spectral moments using point (i) (W energy), we get:

$$H_S = 0.0212 U_0$$

$$T_e = 0.625 U_0$$

These parameters specify significant wave height and wave period (wave energy) for any given wind speed.

Particular application:

In the article of Harrison and Wallace (2005), a wave energy appraisal is conducted, using a Wave Energy Converter developed by Edinburgh-based Ocean Power Delivery Ltd[1] (Surface-following attenuator). The Pelamis is a 120 m long floating device that resembles a sea-snake with four articulated sections that flex (and produce up to 750 kW) as waves run down the length of the device. It is designed to maximize production in normal sea conditions whilst surviving heavy seas (HS>8 m) through power limitation.

Considerations for integration in the CDS toolbox

ERA5 daily and monthly averaged data on single levels from 1979 to present

2.1.3 Solar Technology

With a solar panel a cell converts sunlight directly into electricity. When photons (particles of sunlight) hit solar panels, the panel turns the photons it receives into electrons of direct current electricity. The inverter then converts the direct current electricity into alternating current power, which can be used to power appliances.
The performance of PV systems is largely influenced by internal and external factors such as its structural features, visual loss, aging, radiation, shading, temperature, wind, pollution, and electrical losses. Climate change will impact temperature and irradiance and therefore will alter the output capacity of PV systems.

2.1.3.1 Solar radiation, temperature, wind

- **Climate impact**

Solar panels' efficiency is affected by solar radiation. In a way, it is linked with clear-sky radiation and cloud cover. If a PV panel is exposed to too high temperatures (hence, higher radiation), it loses efficiency and even sometimes, when it is cloudier, efficiency increases. (Jerez, et al., 2015; Flowers, et al., 2016).
PV systems present a negative linear relationship between the energy output and the temperature change, while the increase of solar radiation is proportional to the PV energy output. (Panagea, Tsanis, Koutroulis, & Grillakis, 2014)

- **Summary of results**

From our literature review, for air temperature, an increase of 1˚C would decrease solar PV efficiency by 2% for the most pessimistic study and by 0.5% per 10˚C increase for the optimistic

[1] http://www.oceanpd.com/

one. Concerning irradiance, an increase of 1 unit (W/m^2) will increase solar output by 5%. Finally for wind, an increase of speed by 1m/s will lead to an increase of efficiency of 0.5%.

- **Results**

Good and Calaf (2019) found that Solar PV efficiency diminishes as a function of air temperature at a rate of approximately 0.5% per 10 °C. Light winds lead to increased energy efficiency relative to quiescent conditions with a 0.5% increase in efficiency from 0.5 m/s to 1.5 m/s.

In Greece, Panagea et al. (2014) found regional differences but on average, the individual increase of 1 unit in irradiance results in a significant increase on PV energy output up to 5% while the increase of one unit of temperature causes a decrease up to 2% on the solar PV efficiency.

- **Methodology**

Method 1 (Photovoltaic Softwares, 2020)

The global formula to estimate the electricity generated in output of a photovoltaic system is:

$$E = A * r * H * PR$$

E: Energy (kWh)
A: Total solar panel Area (m2)
R: solar panel yield or efficiency (%) given by the ratio = electrical power (in kWp) of one solar panel divided by the area of one panel.
H: Annual average solar radiation on tilted panels (shadings not included). You have to find the global annual radiation incident on your PV panels with your specific inclination (slope, tilt) and orientation (azimut) with Unit = kWh/m2.
PR: Performance ratio, coefficient for losses (range between 0.5 and 0.9, default value = 0.75).It is a very important value to evaluate the quality of a photovoltaic installation because it gives the performance of the installation independently of the orientation, inclination of the panel. It includes all losses.

Example: the solar panel yield of a PV module of 250 Wp with an area of 1.6 m2 is 15.6%. This nominal ratio is given for standard test conditions (STC): radiation=1000 W/m2, cell temperature=25 Celsius degree, Wind speed=1 m/s, AM=1.5. The unit of the nominal power of the photovoltaic panel in these conditions is called "Watt-peak" (Wp or kWp=1000 Wp or MWp=1000000 Wp).

Considerations for integration in the CDS toolbox

ERA5 monthly: 'mean_surface_downward_short_wave_radiation_flux' (W/m2)
CMIP5 monthly: 'surface_solar_radiation_downwards'(W/m2)

Method 2 (Gomes, Diwan, Bernardo, & Karlsson, 2014)

The efficiency of a PV-system is almost independent of the solar irradiance, while on solar thermal systems the efficiency is strongly dependent. The efficiency of a thermal collector is often zero at low light intensities.

Values were chosen in order to represent standard market panels. Thus the PV panel has an efficiency of 15% and the solar thermal collector has a maximum efficiency of 80%, and a total U value of 4 with $\Delta T = [T_{med} - T_{amb}] = 50ºC$ which was considered to be frequent. The graphics (see Figure 4) are drawn according to a simplified model using the following formulas:

Figure 4 Effect of solar radiation on the power and efficiency PV panels and solar thermal collectors

For PV panels: $P = I * \eta$ (1)

$\eta = 15\%$ (2)

For solar thermal collectors: $P = \eta_0 * I - U * \Delta T$ (3)

$\eta = P / I$ (4)

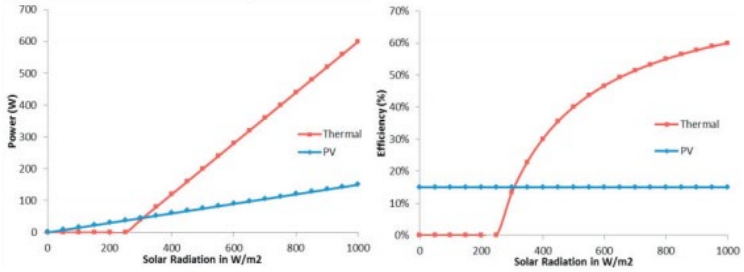

As indicated above, there are more factors to consider, such as the fact that the temperature of the solar cells will increase together with the solar radiation, which will lead to a decrease in solar cell efficiency.

This means that the efficiency of the PV collector is not a straight line as shown but decreases with solar radiation following a coefficient of around 0.45%/ºK for mono crystalline solar cells.
In the same manner, the PV power curve will continue to increase with solar radiation but the real curve is less steep than that shown above. However, the efficiency of solar cells is also increased for higher radiations which compensates for this effect.

Considerations for integration in the CDS toolbox

Solar radiation (J/m^2): ERA5 monthly averaged and hourly data on single levels from 1979 to present

Ambient and median temperature (K): ERA5-Land monthly averaged and hourly data on single levels from 1981 to present

Method 3 (Panagea, Tsanis, Koutroulis, & Grillakis, 2014)

1. Estimation of PV Energy Output under Variable Conditions of Temperature and Irradiance

In order to calculate the potential percentage change in PV output, the fractional change $\Delta P_{PV}/P_{PV}$ is calculated from the ratio between (2) and (3) taken from *Crook et al.*[2] *(refer to it for all equations).* RCM temperature and irradiance outputs were corrected for their biases in mean and standard deviation for each calendar month, following the methodology presented in an article by Haerter et al. (2011).

Consider the following:

$$\begin{aligned}\frac{\Delta P_{PV}}{\eta_{ref}} &= -\Delta T G_{tot}\beta c_2 + \Delta G_{tot}\left(1 - \beta c_1 + \beta T_{ref} - 2\beta c_3 - T\beta c_2\right) \\ &\quad - \Delta G_{tot}^2 \beta c_3 - \Delta G_{tot}\Delta T \beta c_2 + \Delta G_{tot}\gamma \log_{10}\left(G_{tot} + \Delta G_{tot}\right) \\ &\quad + G_{tot}\gamma \log_{10}\left(\frac{G_{tot} + \Delta G_{tot}}{G_{tot}}\right),\end{aligned} \tag{2}$$

$$\frac{P_{PV}}{\eta_{ref}} = G_{tot}\left(1 - \beta\left(c_1 + c_2 T + c_3 G_{tot} - T_{ref}\right) + \gamma \log_{10} G_{tot}\right), \tag{3}$$

Where:

ΔP_{PV} is the change in photovoltaic power output

η_{ref} is the reference photovoltaic efficiency

ΔT is the change in temperature between the baseline and the scenario period

ΔG is the change in irradiance between the baseline and the scenario period

T is the daytime temperature for the baseline period, estimated by (4) as it can be found in *Crook et al.*

G_{tot} is the irradiance over the daylight for the actual cloud cover for the baseline period, calculated by (5) taken from *Crook et al.*

T_{ref} is the reference temperature in which the performance of PV cell is estimated by the manufacturer

β is the temperature coefficient set by cell material and structure

γ is the irradiance coefficient set by cell material and structure

[2] J. A. Crook, L. A. Jones, P. M. Forster, and R. Crook, *"Climate change impacts on future photovoltaic and concentrated solar power energy output,"* Energy and Environmental Science, vol. 4, no. 9, pp. 3101–3109, 2011

$c1$, $c2$, and $c3$ are coefficients which depend on details of the module and mounting that affect heat transfer from the cell.

2. Daytime temperature

$$T = \overline{T} + \frac{\overline{\mathrm{DTR}}}{4}, \qquad (4)$$

DTR is the diurnal range of the temperature (difference between minimum and maximum temperature) and T is the monthly average temperature.

3. Irradiance

$$G_{\mathrm{tot}} = \overline{G}\frac{t_{24\mathrm{h}}}{t_{\mathrm{daylength}}}, \qquad (5)$$

G is the monthly average irradiance, $t_{\mathrm{daylength}}$ is the time of the daylight, calculated as monthly average, for all latitudes of the study site every 0.25∘.

Considerations for integration in the CDS toolbox

Temperature (K): Temperature statistics for Europe derived from climate projections

Irradiance:

1. Dimensionless: Surface albedo 10-daily gridded data from 1981 to present
2. W/m^2: Climate data for the European energy sector from 1979 to 2016 derived from ERA-Interim

Method 4 (Adeh, Good, Calaf, & Higgins, 2019)

The results of this study confirm that the PV panel efficiency is influenced by the solar radiation, air temperature, wind speed and relative humidity. The solar PV potential fundamentally depends on the incoming solar radiation, which is strongly dependent on geographic location, but it is also well-known that the system's efficiency depends on the temperature of the solar cells, and the temperature of the solar cells is a function of the local microclimate.

1. Energy Balance

Steady state is assumed, and the atmosphere is modeled under a neutral stratification as a first order approximation. The consequence is that the energy storage term is neglected and that the ground temperature is equal to the air temperature. The resultant energy balance of the panel is expressed as:

$$(1-\alpha-\varepsilon)R_{\downarrow}^{sun}+L_{\downarrow}^{sky}+L_{\uparrow}^{g}-2L^{p}-2q_{conv}=0,$$

Where **ε** is the efficiency of the solar panel, **α** = 0.2 is the PV panel surface albedo**,** R^{sun} is the measured incoming shortwave radiation from the sun.

Particular application: Oregon, USA (Adeh, Good, Calaf, & Higgins, 2019)

The microclimate-informed PV efficiency model is validated using field data[3] from a 1.5 MW solar array located at Oregon State University in Corvallis, Oregon[4]. Climatic variables (temperature, relative humidity, wind speed and incoming short-wave radiation were collected at a height of two meters (as the solar panel height) and one-minute intervals over two years Impact of air temperature, wind speed and vapor pressure are available in boxplot format. We cannot assess a precise result due to standard deviation and confidence intervals but nonetheless tendencies are clear. Air temperature has a linear decreasing impact on panel efficiency. Wind speed is more spurious but seems to have a decreasing return to scale tendency. Finally, regarding vapor pressure, we cannot stipulate any clear tendency.

The following equation is was used:

$$\varepsilon=\varepsilon_{ref}\left[1-A\left(T_p-T_{ref}\right)\right],$$

Where ε_{ref} = 0.135, is the reference efficiency of the panel at a reference temperature, T_{ref} = 298 K, and A=0.0051/°K is the change in panel efficiency associated with a change in panel temperature. Tis linear relationship is assumed valid when the absolute value of $[T_p - T_{ref}] \leq 20$ °K.

Night time periods and times of low sun angles (≤15°) were excluded from the analysis. In the global scale analysis, the input environmental data were provided for each 0.5°×0.5° pixel.

Considerations for integration in the CDS toolbox

- Albedo (Dimensionless): ERA5-Land monthly averaged data from 1981 to present
- Irradiance (W/m^2): Climate data for the European energy sector from 1979 to 2016 derived from ERA-Interim
- Radiation (W/m^2): ERA5 monthly averaged data on single levels from 1979 to present
- Air temperature (K): ERA5 monthly averaged data on single levels from 1979 to present

[3] Adeh, E. H., Higgins, C. W. & Selker, J. S. *Remarkable solar panels Influence on soil moisture, micrometeorology and water-use efficiency-database* (2017)

[4] Adeh, E. H., Selker, J. S. & Higgins, C. W. Remarkable agrivoltaic influence on soil moisture, micrometeorology and water-use efficiency. *PloS One* **13**, e0203256 (2018).

2.1.3.2 Dust and ash

- **Climate impact**

Dust and ash deposition on the PV cells reduces efficiency of solar panels because they impede panels to totally absorb solar radiation and hence, energy produced decreases.

- **Summary of results**

The impact of dust accumulation on solar PV efficiency is -1.5% per 0.4mg/cm^2. We also find that efficiency decreases by 7% for any dust accumulation. For power output, the decrease is in the range [2.5%; 30%; 84%] for dust accumulation in mg/cm^2 of [0.06; 0.4; 25].

- **Results**

In a study done by Kaldellis & Fragos (2011), a considerable deterioration of the PV-panels' performance is obtained, i.e. almost 30% energy reduction per hour or 1.5% efficiency decrease (in absolute terms) for ash accumulation on the panels' surface reaching up to 0.4 mg/cm^2. Even a relatively small ash deposition (i.e. 0.06 mg/cm^2) may cause almost 2.5% reduction in the generated power output.

Furthermore, the effects of dust accumulation on PVs' surfaces have been experimentally investigated by El-Shobokshy and Hussein (1993), aiming to relate the dust deposition density with the short circuit current and power output variation. According to the results obtained, atmospheric dust particles, with a mean diameter of 80 mm, may reduce the PV-panel's short circuit current and the power output by about 82% and 84%, respectively, when the dust deposition density is almost 250 g/m^2.

To determine the relation of natural dust deposition on PVs' surfaces with the corresponding voltage output under various PV-panels' tilt angles, Kappos et al. (1996) showed that the particle deposition is directly proportional to the inclination of the PV-panel. Particularly, for the vertically placed PV-modules, the mean decrease of the PV voltage output after three months of observation was 5% in contrast to the respective 20% for the PV-modules placed horizontally.

Finally, Meral and Dincer (2011) estimated for a "100 MW solar panel" that the impact of dust is typically on factor reduction of 0.93. A manufacturer may rate a particular PV module output at 100W of power under standard test conditions, and call the product a "100W PV module."

Example: Output power of the PV module reduces as module temperature increases. When operating on a roof, a PV module will heat up substantially, reaching inner temperatures of 50–75 ◦C. For crystalline modules, a typical temperature reduction factor recommended by the CEC is 89% or 0.89. So the "100-W module will typically operate at about 95W× 0.89 = 85W under full sunlight conditions". Concerning dust, a typical annual dust reduction factor to use is 93% or 0.93. A "100- W module," may operate on average at about 85W× 0.93 = 79W. (Meral & Dincer, 2011)

2.1.4 Hydropower Technology

Hydropower is using water that is constantly moving through a vast global cycle which is an endless and constant recharging system that can be used to produce electricity.
When flowing water is captured and turned into electricity, it is called hydroelectric power or hydropower. There are several types of hydroelectric facilities; they are all powered by the kinetic energy of flowing water as it moves downstream. Turbines and generators convert the energy into electricity, which is then fed into the electrical grid to be used in homes, businesses, and by industry.

2.1.4.1 Stream Flow

- **Climatic impact**

Stream flow is a component of the water cycle as it depends on precipitation, runoff and sun mainly. The stronger the stream flow is, the more power a hydropower plant is able to produce.

- **Summary of results**

For RCP 4.5 and RCP 8.5 scenarios, annual energy production would decrease in the range of 6.1% - 58.6%. We also learn that a 1% change in river discharge would result in a 1% change in power generation.

- **Results**

In southeast Brazil, in the Grande river basin region, De Oliveira et al. (2017) found out that in general, based on their baseline period (1961-2005) and scenarios (RCP 4.5 and 8.5, 2007 – 2099), stream flow will decrease and lead to reductions in hydropower potential and hence decreases of the annual energy production varying from 6.1 to 58.6% throughout the 21st Century.

From an article of the US Department of Energy (2008), we learn that the sensitivity of hydroelectric generation to changes in precipitation and river discharge is high: a 1 percent change in precipitation or river discharge typically results in 1 percent change in generation (ORNL, 2007).

- **Methodology**

Method 1 (De Oliveira, De Mello, Viola, & Srinivasan, 2017)

The SWATmodel taken from Ulrich and Volk (2009) was used to simulate the hydrological behavior of the headwaters under the Representative Concentration Pathways 4.5 and 8.5 scenarios.

Hydropower potential:

$$N_P = Q \times H \times \rho_w \times g \times \eta \qquad (6)$$

where N_P is the hydropower potential (W); Q is the stream-flow ($m^3 s^{-1}$); H is the hydraulic head (m); ρ_w is the water density ($kg\,m^{-3}$); g is the gravitational acceleration ($m\,s^{-2}$); and n is the total plant efficiency.

Considerations for integration in the CDS toolbox

- Water quantity indicators for Europe
- CDS API ONLY: River discharge and related historical data from the Global Flood Awareness System

Method 2 (Eliasson & Ludvigsson, 2000)Produced Power:

$$F_{re}(t) = \gamma\, Q(t)\, H_{br}$$

F_{re}	Produced power
Q(t)	Flow through the station.
H_{br}	Gross head
γ	Unit weight of water
t	time

Method 3 (Engineering ToolBox, s.d.)

The practically available power is estimated as follows:

$P_a = \mu\, \rho\, q\, g\, h$ (2)

where

P_a = power available (W)

μ = efficiency (in general in the range 0.75 to 0.95)

ρ = density (kg/m^3) (~ 1000 kg/m^3 for water)

q = water flow (m^3/s)

g = acceleration of gravity (9.81 m/s^2)

h = falling height, head (m)

Considerations for integration in the CDS toolbox

Water quantity indicators for Europe

2.1.4.2 Precipitation / Run-off

- **Climate Impact**

Precipitation influences hydropower generation through water availability. If there are droughts, water quantity may be insufficient to generate electricity, or for a hydropower plant to operate at full capacity.

Runoff is the result of the incapacity of the soil to absorb or contain high levels of water. When water is not absorbed, it is conveyed into rivers, hence becoming usable for hydropower stations.

- **Summary of results**

We found that a 1% change in precipitation would imply a 1% change in power generation.

- **Results**

In the Zambezi River Basin, Yamba et al. (2011) found out that future power potential will fluctuate over time (2010-2070). It is forecasted that between 2010 and 2030 there will be a decrease, then a partial recovery between 2030 and 2050 to finally see a more marked decline until 2070.

In the US, the US Department of Energy and Department of Homeland Security indicates that the sensitivity of hydroelectric power generation to changes in precipitation and river discharge is high; in the range of 1.0+ which means that a sensitivity level of 1.0 means that one percent change in precipitation results in one percent change in power generation (Choi, Keith, Hocking, Friedman, & Matheu, 2011).

- **Methodology**

Method 1 (Yamba, et al., 2011)

1. Precipitation

$$P = Q + E \pm S \pm G$$

P precipitation or rainfall
Q surface and subsurface run-off
E evapo-transpiration losses
S change in soil moisture
G change in groundwater, (Pitman, 2001)

2. Efficiency

$$P_{Gross} = \frac{\rho_{WATER} * g * H_{GROSS} * Q}{10^6}$$

P_{Gross}	gross power (MW)
ρ_{WATER}	density of water (kg/m^3)
G	acceleration due to gravity (m^2/s)
H_{GROSS}	gross head (m)
Q	annual run-off into the reservoir (m^3/s)

Considerations for integration in the CDS toolbox

- ERA5-Land monthly averaged and hourly data from 1981 to present
- Soil moisture gridded data from 1978 to present

2.1.5 Gas Power

Natural gas is a product of decomposed organic matter, typically from ancient marine microorganisms, deposited very deep into soils. After natural gas forms, it will tend to rise towards the surface through pore spaces in the rock. This gas is then mixed with air for combustion and through the use of turbines, it will generate electricity.

Gas turbines in power stations are composed of three parts: the compressor which draws air into the engine; the combustion system where the natural gas is mixed and combusted with air; the turbine where the hot combustion gas comes and rotates the blades.

In the next sections ISO, or standard reference conditions are cited, which are conditions on levels for ambient air temperature (15˚C), atmospheric pressure (101.32 kPa) and air relative humidity (60% %) to determine the efficiency of thermal power generation.

2.1.5.1 Air Temperatures

- **Climate impact**

Gas turbine power output increases when it is cold, and decreases when it is hot. This is due to the following:

- A gas turbine is a fixed volume machine. You can only squeeze a fixed volume of air through the compressor and turbine.
- The density of air increases when it is cold. Colder air means more mass of air in the same amount of volume.
- The amount of power generated in the turbine increases with a higher mass of air flowing through the turbine.

Ambient temperature also has an effect on the compressor. Colder air improves compressor efficiency. This means that the compressor consumes less power, leading to more power supplied to the generator (Green, 2020).

- **Summary of results**

From our literature it emerges that for air temperature range [+1˚C; +5.56˚C (10˚F); +10˚C (10K); +35˚C], the impact on gas power plant output (decrease) is of [0.12-0.45% and 0.5%-0.9% on average; 3-4%; 5-10%; 24%] respectively.
For absolute values, two of our references state a decrease in MW with values of [1.47; 2.4] for an increase in temperatures of order [+1˚C; +5.56˚C (10˚F)] respectively.

- **Results**

In the US (East-Coast for most of plants), Maulbetsch and Di Filippo (2006) estimated output regarding ambient temperature for wet- and dry-cooled plants (see Figure 5 and Figure 6). A marked decline in efficiency can be observed, especially for dry-cooled power plants.

Figure 5 Output vs. ambient temperature (wet-cooled plants)

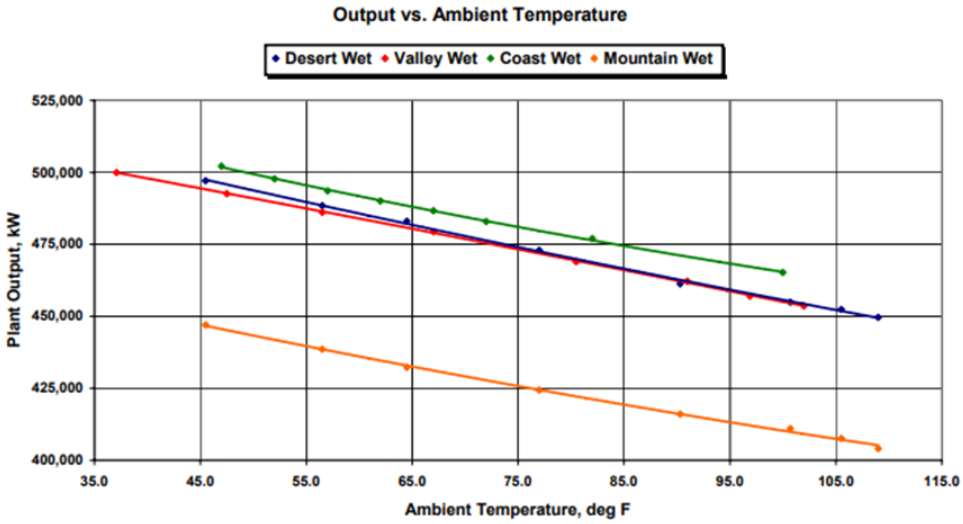

Figure 6 Output vs. ambient temperature (dry-cooled plants)

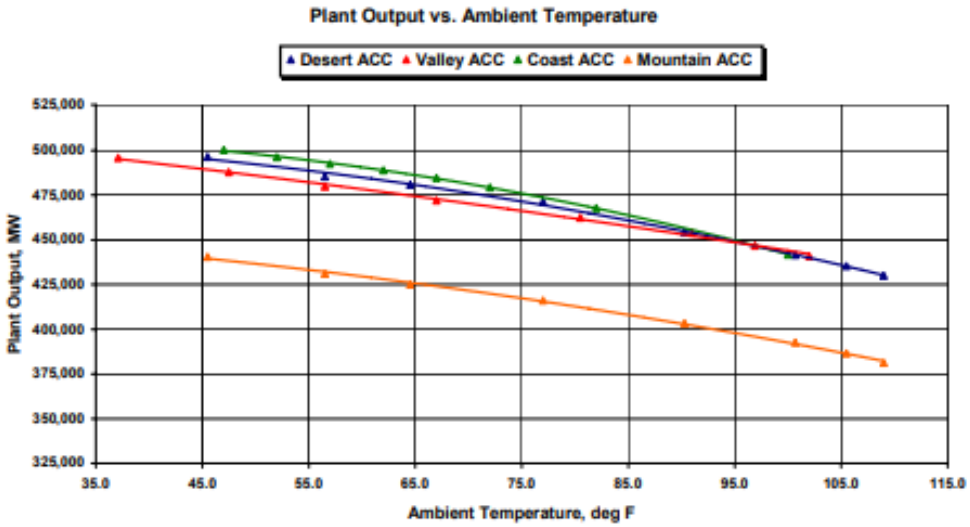

In Dubai, De Sa and Al Zubaidy (2011) compared efficiency relative to ISO conditions and found that for every Kelvin (K) rise in ambient temperature above ISO conditions the Gas Turbine loses 0.1% in terms of thermal efficiency and 1.47 MW of its Gross (useful) Power Output (see Figure 7, Figure 9 and Figure 8).

Figure 7 Gas turbine power and efficiency in relation to ambient temperatures

Gas turbine power and efficiency at ambient temperatures different from ISO condition.

Model	SGT 94.3						
GT Inlet Temp (Ambient)	K	15	21.59	26.26	35.44	40.84	46.72
GT Power Output	MW	265[a]	257.39[a]	247.96[a]	235.8[a]	227.7[a]	220.35[a]
GT Thermal Efficiency	%	37	33.96	33.72	32.58	32.38	32.26
Decrease in Power Output with respect to ISO GT Inlet temperature (15 K)	%	0	2.87	6.43	11.02	14.08	16.85
Decrease in Thermal Efficiency with respect to ISO GT Inlet temperature (15 K)	%	0	8.21	8.86	11.94	12.48	12.81

[a] Operation of Gas Turbine with Hydraulic Clearance Optimization (HCO) active.

Figure 8 Thermal efficiency and Power variance

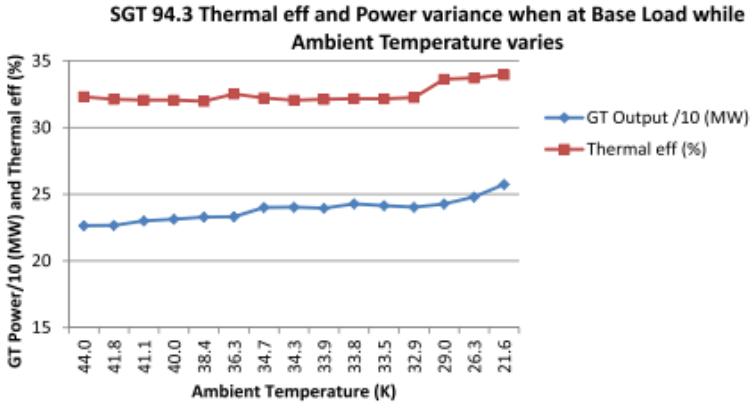

Fig. 5. The behavior of gas turbine SGT 94.3 thermal efficiency and power variance when at base load at varying ambient temperature during the annual continuous monitored period.

Figure 9 Thermal efficiency and ambient temperature

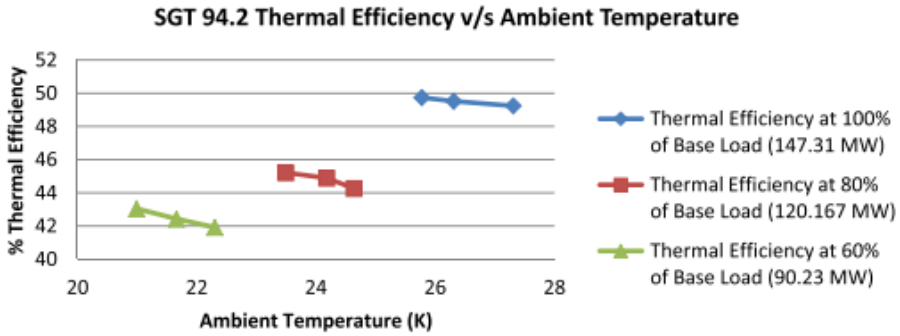

Fig. 4. Behavior of gas turbine SGT 94.2 thermal efficiency under various operating loads at varying ambient temperature during the performance tests.

In Greece, Kakaras et al. (2006) found that depending on the gas turbine type, power output is reduced by a percentage between 5% and more than 10% of the ISO-rated power output 15°C for every 10K increase in ambient air temperature (see Figure 10).

Figure 10 70 MWe (a) and 40 MWe (b) gas turbines output and efficiency related to air temperatures

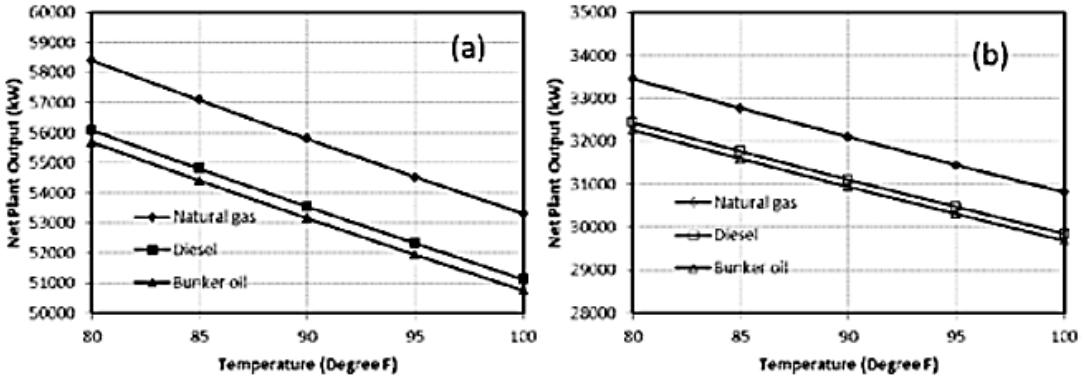

Fig. 3. Effect of temperature on net plant output [for gas turbine frames (a) GE 70 MW_e GE6101FA, (b) GE 40 MW_e GE6561B, Humidity 30%].

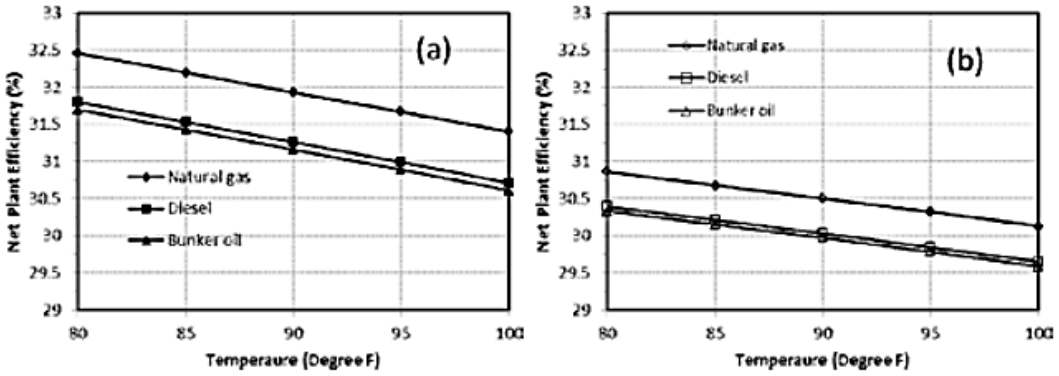

Fig. 4. Effect of temperature on net plant efficiency [for given gas turbine frames (a) GE 70 MW_e GE6101FA, (b) GE 40 MW_e GE6561B, Humidity 30%].

In Saudi Arabia, Basha et al. (2011) showed that in absolute terms, plant net output from a 70 MWe gas turbine frame using natural gas has been found to increase from 53.3 to 55.7 MWe for a decrease in temperature by 10 °F.

In Vietnam, for a particular application, it is said that there is an approximate 0.57% decrease in power output for each degree increase in air temperature (Asian Development Bank, 2012). It may appear peculiar that power output decreases over the entire range of temperature while net efficiency increases up to 29˚C (see Figure 11). With a gas turbine, power output and energy efficiency decrease as air temperature increases. On the other hand, with a steam turbine, air temperature increase leads to a rise in exhaust gas temperature, which in turn improves the power output and efficiency of the steam turbine. The CCGT O Mon IV power plant has a configuration of 2-2-1: two gas turbines each with a power output of 260–290 MW, two heat recovery steam generators with a capacity of 714 tons/h, and one steam turbine with a power output of 264–289 MW. A decrease in the output of the gas turbines would have caused greater impact to the system than the increase in the output of the steam turbine. Since gas turbines represents 2/3 of the overall power output from O Mon IV, overall output decreases with temperature increase.

Figure 11 Plant efficiency and power output vs. air temperature

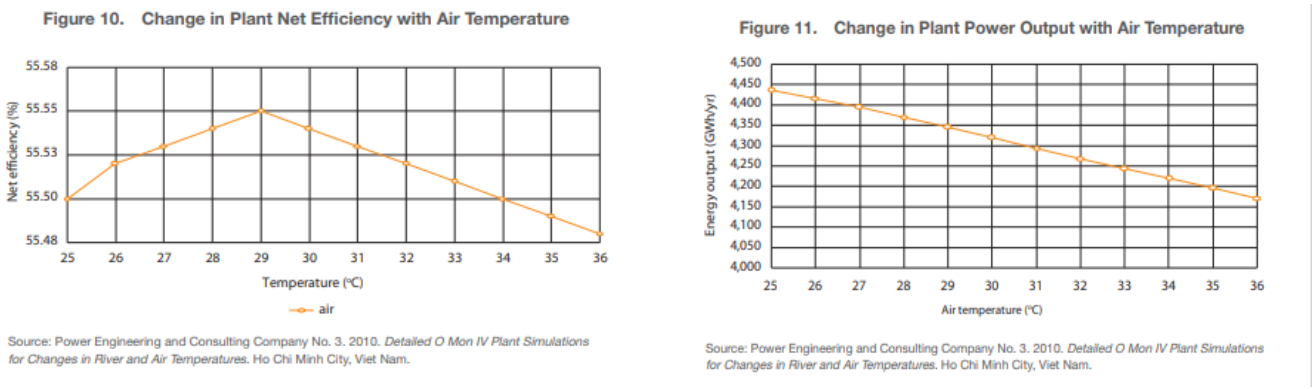

Petchers (2003) arrived at the conclusion that for every 1˚C increment in the ambient temperature the amount of the reduction in power output is nearly 0.9%. With the increase of the ambient temperature the density of the air decreases. Consequently, the air mass flow rate into the turbine decreases and so the gas turbine power output reduces (see Figure 12).

Figure 12 Ambient Temperature Power Correction Factor Curve

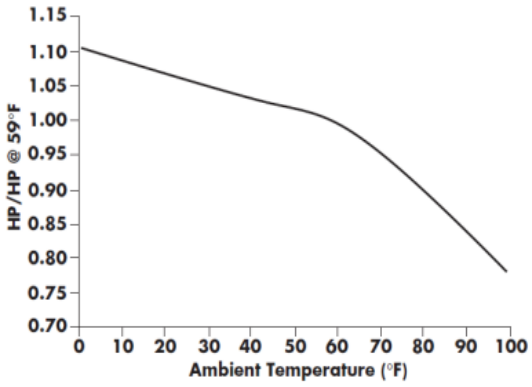

Figure 3: Ambient Temperature Power Correction Factor Curve (Petchers, 2002)

Shukla and Singh (2014) affirmed that the gas turbine output is a strong function of the ambient air temperature with its power output dropping by 0.5-0.9% for every 1˚C increase in ambient temperature (see Figure 13).

Figure 13 Thermal efficiency vs. Air temperature

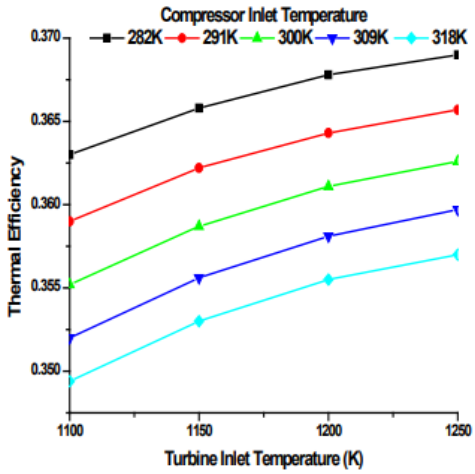

Finally, Ghamami et al. (2016) estimated that for one degree Celsius rise in temperature ambient air, intake and exhaust gas temperature of the turbine by an average of 0.4 degrees Celsius, respectively 0.17 ° C decrease and increase (see Figure 14).

Figure 14 Gas turbine exhaust gas temperature changes graph input and ambient temperature

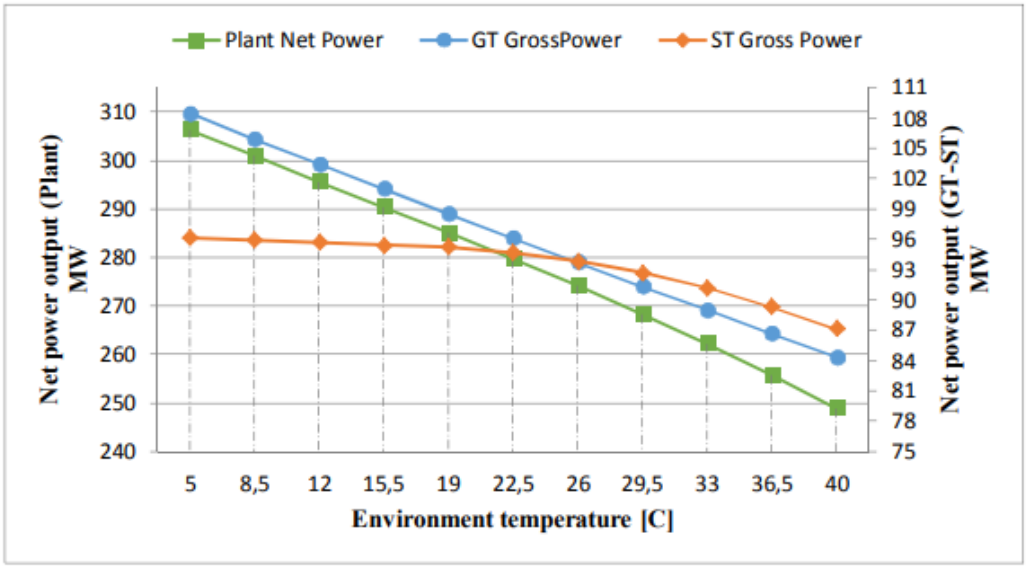

On the other hand, it is worth mentioning that impacts vary, and other factors have to be considered. For instance, Henry and Pratson (2016) criticize studies that predict that droughts and hotter water and air temperatures caused by climate warming will reduce the efficiency (η) of thermoelectric plants, specifically citing the range 0.12−0.45% for each 1 °C of warming. The article precises that efficiency and power output are not significantly correlated, and magnitude is lower than assumed. They indicate that efficiency and power output depend also on the plant attributes such as age, nameplate capacity, fuel type, average heat rate, and location.

In a specific case study elaborated by Singh and Kumar (2012), in estimating the impact of air temperature change impact on a specific plant, they find that a 11% decrease in the mass flow rate of air is caused by the increased in ambient air temperature from 5 to 40˚C. Following the same changes in AAT, net power output from the gas turbine decreases by 24% and plant efficiency by 9%. Power output from a steam turbine is found to decrease by 9%. Also the mass flow rate of steam is decreased by 10%.

According to a report of Acclimatise (2009)there is a linear relationship between air temperature and turbine efficiency: a 10 degree Fahrenheit (5.56˚C) increase in ambient temperature would produce as much as a 3-4% reduction in power output (also valid for coal power plants).

- **Methodology**

Method 1 (Maulbetsch & Di Filippo, 2006)

Relative EGP = 1 - (MAX (0, "Td" - "2.7") * "0.21")/100

Relative EGP = relative efficiency of gas-powered generation
2.7 = the lowest temperature in the Maulbetsch study
Td = daily temperature
0.21 = the percent reduction in efficiency per °C

Considerations for integration in the CDS toolbox

- 2m Temperature: ERA5 monthly data
- 2m Temperature: CMIP5 monthly data

Method 2 (Asian Development Bank, 2012)

Particular application to a project and established power plant named O Mon IV, located in Vietnam.

The net plant efficiency under the PECC3 simulations peaked at 29°C, and then exhibited a gradual linear decrease in efficiency with further increases in temperature. This relationship can be approximated as linear for temperatures greater than 29°C, with a 0.01% decrease in efficiency with each 1°C increase in temperature. Power output of O Mon IV showed a strong and decreasing linear trend (R2 = 0.999) according to the equation:

$$P(T) = -24{,}54T + 4465{,}6$$

Where P (T) is energy output measured in GWh/year. Based on this trend, there is an approximate 0.57% decrease in power output for each degree increase in air temperature.

Considerations for integration in the CDS toolbox

Temperature (K): ERA5-Land hourly data from 1981 to present

2.1.5.2 Ambient Pressure

- **Climate impact**

With the increases of elevation, the density of the air reduces, thus ambient pressure reduces and thus, has a negative impact on gas power output.

- **Results**

Petchers (2003) estimated that as a result of mass flow rate, fuel rate and the power output of the gas turbine reduce nearly by 3.5% for each 1000 feet (305m) of elevation above the sea level (see Figure 15).

Figure 15 Power output relative to elevation

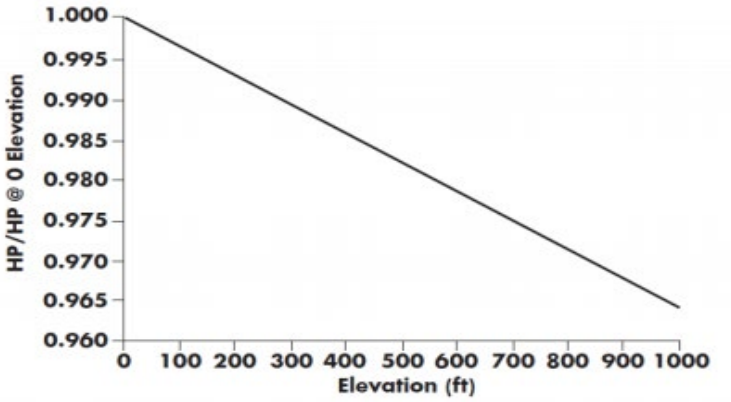

Figure 5: Representative Altitude Power Correction Factor Curve

2.1.5.3 Humidity

- **Climate impact**

Humidity is related to air temperature and so in general, lower temperatures imply more humidity and so better efficiency of the gas power plant.

- **Summary of results**

We observe that there is a +0.65% in thermal efficiency for every +15% relative humidity. At ambient condition of 60˚C, having relative humidity of 100% leads to -1% in efficiency and +25% in specific work output.

- **Results**

Jabboury and Darwish (1990) found that a decrease of 1% in efficiency and an increase of 25% in specific work output were observed when operating at an ambient condition of 60°C and 100% relative humidity over that of 60°C and 0% relative humidity (see Figure 16).

This shows the reason for injecting steam in the compressed air before the combustion chambers in some experiments to increase the power output.

Figure 16 Efficiency vs. Relative humidity for TIT = 1200 K and PR = 10

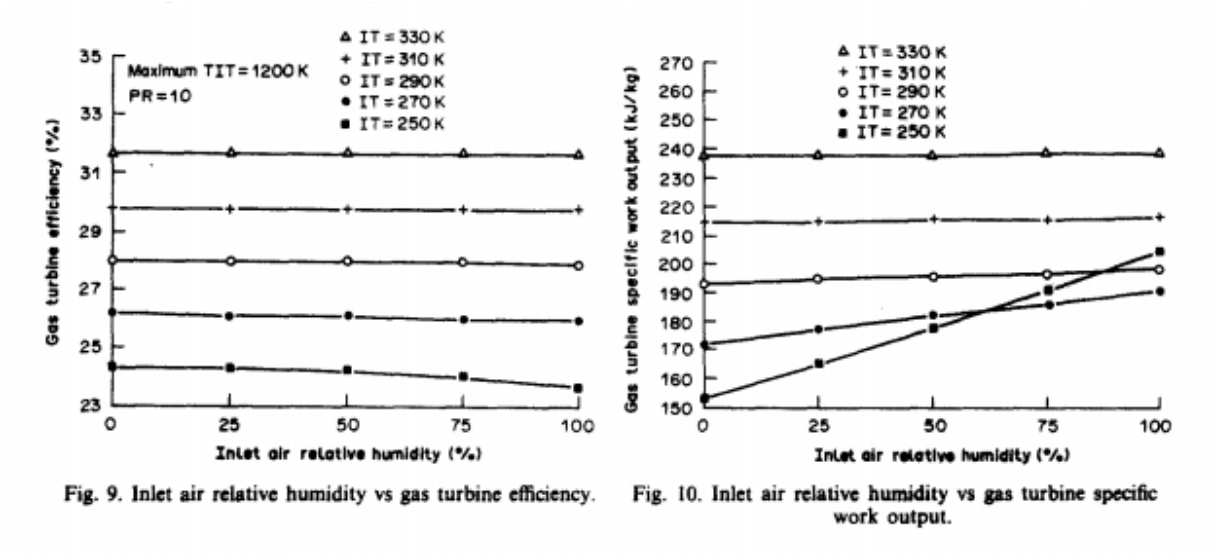

Fig. 9. Inlet air relative humidity vs gas turbine efficiency.

Fig. 10. Inlet air relative humidity vs gas turbine specific work output.

In another article, Shukla and Singh (2014) said that thermal efficiency increases with increase in relative humidity from 0 to 100 percent for a particular CIT. There is 0.65 percent increase in thermal efficiency for every 15 percent increase of relative humidity (see Figure 17).

Figure 17 Variation of thermal efficiency of GT power cycle with different relative humidity at TIT 1100K & CPR 8

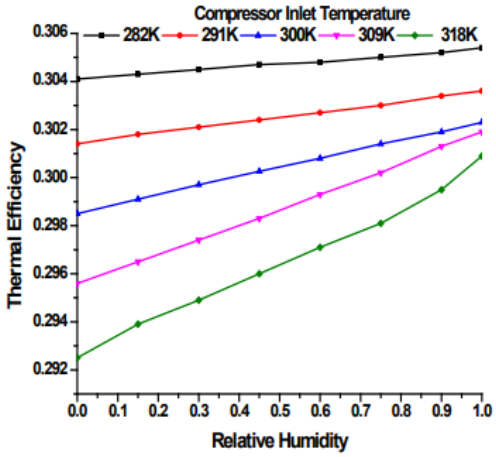

Considerations for integration in the CDS toolbox

- ERA5 single level hourly data from 1981 to present

2.1.5.4 Water temperature

- **Climate impact**

Increasing water temperature has a negative impact on the cooling system, mainly in CCGT (Combined-cycle Power Plant).

- **Results**

In a report based in Vietnam, the Asian Development Bank (2012) estimated that based on their analysis, annual power output in 2040 could be reduced by 25.3 GWh due to changes in river water temperature alone, representing a 0.6% reduction in power output. Net efficiency could also decrease by 0.3%, down to 55.2%.

- **Methodology**

Figure 18 below shows the relative efficiency as a function of river water temperature. For river water temperatures greater than 25˚C, there is an approximately parabolic relationship between water temperature and efficiency, expressed by the following equation (Asian Development Bank, 2012):

$$\varepsilon = -0.006\ T_{river}^2 + 0.2988\ T_{river} + 51.96$$

where T_{river} is the river water temperature in degrees Celsius.

Figure 18 River water temperature impact on energy output

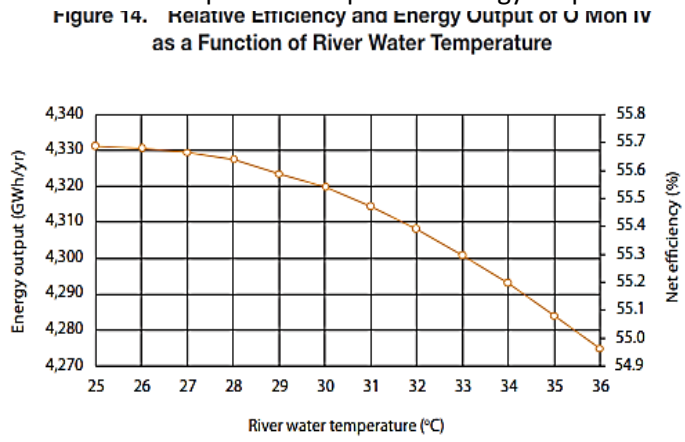

Source: Power Engineering and Consulting Company No. 3. 2010. *Detailed O Mon IV Plant Simulations for Changes in River and Air Temperatures.* Ho Chi Minh City, Viet Nam.

Considerations for integration in the CDS toolbox

Water quantity indicators for Europe

2.1.6 Coal Power

It is reported that more than half electricity produced in the world is from Coal. In order to extract energy from coal, power plants have to burn it in furnaces to produce heat to extract carbon and oxygen that, combined, will produce carbon dioxide and heat. Then, the heat is used to boil water to produce steam at high pressure and temperature which is then piped into turbines that rotate and generate electricity.

Coal power plants are subject to climate risks that would affect their production efficiency in about the same order than other power plants. Some of the impacts are similar to gas power plants.

Many of the results shown below apply also to gas and nuclear power plants.

2.1.6.1 Precipitation

- **Climate impact**

Precipitation has an impact on coal power plants through soil moisture. In fact, it will also depend on regions and soils characteristics but precipitation plays a big role as it infiltrates soils, that make coal become more humid and hence, power plants will need a higher amount of energy to burn it.

- **Summary of results**

Precipitation increase moisture (hence coal humidity): for each +1% in moisture there is a -4% plant load factor. In one of the studies reviewed, 1048 heavy precipitation events were recorded for one year and their impact on the power distribution network, on average, was of 0.99 outage-hour/year.

- **Results**

In India, Bhatt and Rajkumar (2015) compared inherent soil moisture in addition to surface moisture regarding soil characteristics. Bhatt analyzed the cost of production and efficiency of power generation and estimated that an increase of 1% of total moisture will reduce by 4% the plant load factor.

In Malaysia, Handayani et al. (2019) studied the impact of many climate variables on coal power plants (also nuclear and gas power plants). In 2014 (354 floods), 2015 (19 floods) there has been for Java and Bali, an average 16-outage-hours and 1.7-outage-hours for each affected customer respectively (89,102).

Extreme rain events also impacted the distribution of electricity. Between 2014 and 2015, heavy precipitation caused 1048 events of power outages in the Java-Bali distribution network. These events resulted in 8.3 gigawatt-hour ENS (energy not supplied) that is equal to an estimated loss of more than 0.5 million USD over the two years. Each underwent an annual average of 0.99-outage-hour due to heavy-precipitation-related failures in distribution networks.

- **Methodology**

Decrease in boiler efficiency due to moisture increase (Bhatt & Rajkumar, 2015):

$$Y = -0.02X^2+0.358X+81.87$$

Unit heat rate:

$$Y = 0.631X^2-11.56X+2628$$

Considerations for integration in the CDS toolbox

- Soil moisture gridded data from 1978 to present

2.1.6.2 Air and water temperature

- **Climate impact**

Coal combustion in the boiler requires air. If air temperature increases, density decreases and hence we will need more quantity of air for the combustion. Water is used to extract, wash, and sometimes transport coal; cool the steam used to make electricity in the power plant; and control pollution from the plant. When water temperature increases, cooling of the steam system becomes less efficient and hence the power plant loses efficiency.

- **Summary of results**

As water temperature increase by 1˚C, the impact on coal power plant efficiency is -0.02% (once-through cooling system) and -0.017% (open-loop system).
Air temperature change from a base case (42˚C) of range (˚C) [42; 42.7; 45; 47; 50], has an impact on air pre-heater efficiency change of [89.94; 86.22; 79.99; 77.6; 76.04] respectively and also on overall change in efficiency of [77.29; 73.38; 65.54; 62.43; 55.38] respectively.
Another study without base case, estimated that for each +5˚C there would be a decrease in efficiency of 0.34%.

- **Results**

In the US, in a Master thesis written by Colman (2013), regressions using USGS and NOAA air and water temperature data and EPA records of power plant fuel consumption and power output,

came to the conclusion that a 1° C increase in water temperature is correlated with a 0.02 percentage point decrease in plant efficiency when using a once-through cooling system.
For an open-loop coal power plant, mean water temperature increase of 1˚C effect is of -0.017 reduction in efficiency.
In India, Bhattacharya and Sengputa (2016) estimated the effect of change in ambient air temperature to assess the performance of regenerative air pre-heater with reference to a field study of 135 MWe subcritical steam power plant.
T_{ae} (°C) change [42; 42.7; 45; 47; 50] translated into APH efficiency change η_{APH} (%) [89.94; 86.22; 79.99; 77.6; 76.04] and lately into overall change in efficiency $\eta_{overall}$ (%) [77.29; 73.38; 65.54; 62.43; 55.38].

In a report of the European Commission (2011), Fossil-fueled power plants will be impacted by extreme rise (5˚C – 10 ˚C) in water temperature of seas (for power plants close to shores). There will be the need for additional investments for cooling towers at around 100 euros/kW.

2.1.7 Nuclear Power

The energy generated by a nuclear plant is extracted from atoms energy resulting from a fission process from radioactive isotopes that is made on demand.
Nuclear fission is when a large atom split into one or more smaller atoms, giving off other particles and energy in the process.

A nuclear plant is composed of a nuclear reactor core where there's a generator that produces the energy and the turbine that turns it. Then we have the jet of steam that turns the turbine and finally the radioactive uranium bundle that heats water into steam.

The water in the reactor also serves as a coolant for the radioactive material, preventing it from overheating and melting down

2.1.7.1 Water temperature

- **Climate impact**

The impact of water temperature is important for the cooling systems required by nuclear power plants. If water is too hot, the cooling system won't be efficient and it could result in a decrease of power output, shutdown or even physical damage to the plant.

- **Summary of results**

When compiling all our references and establishing averages and ranges it emerges that an increase of water temperature (in ˚C) of [+1; +5; +10; +15-30] has a negative impact on efficiency of [0.12-0.16%; 0.76-1%; 1.52%; 2.27%]. For power output decrease, it is in the range of [0.39-0.45%; 2.17%; 4.37%; 6.55%]. Also, we found that the summer capacity of a power plant

decreases by 6.3-19% in Europe and 4.4-16% in the US for an increase of water temperature of 1.4-2.4˚C on average.

- **Results**

Ibrahim et al. (2014) estimated that when the cooling water inlet temperature increases by 1°C, 5°C, 10° C, and (15–30°C), the thermal efficiency decreases by 0.16, 0.76, 1.52, and 2.27%, respectively.

He also estimated that the variation of net power output with cooling water inlet temperature. An increase of water inlet temperature of 1°C, 5°C, 10°C, and 10–35°C corresponds to decrease in W_{net} by 0.39293, 2.166, 4.3683, and 6.547%, respectively.

Figure 19 presents the variation of thermal efficiency ηth with cooling water inlet temperature T_{cwi}. Figure 20 presents the net power output W_{net} variation with respect to the cooling water inlet temperature T_{cwi}.

Figure 19 Thermal efficiency vs. water temperature

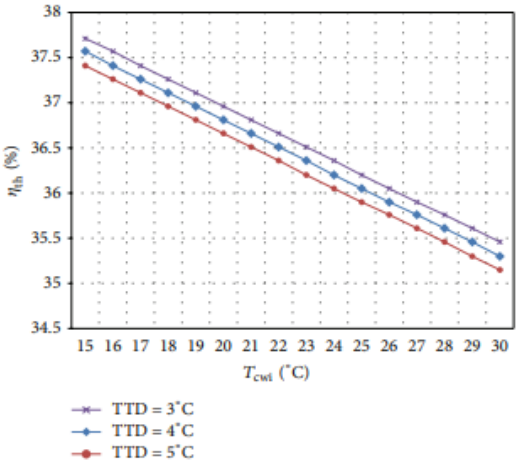

FIGURE 6: Variation of thermal efficiency η_{th} with cooling water inlet temperature T_{cwi}.

Figure 20 Net power output vs. water temperature

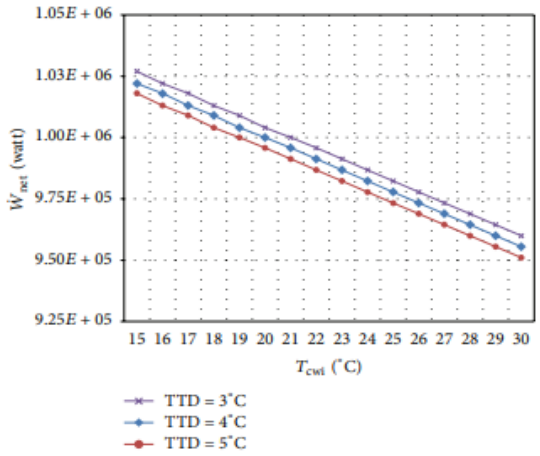

FIGURE 7: Variation of net power output W_{net} with cooling water inlet temperature T_{cwi}.

In another article, Van Vilet et al. (2012) estimated water temperature impact related to Nuclear power plants close to river flows. The performance of the modelling framework was tested for the historical period 1971–2000. Observed daily series of river flow and water temperature for 1,267 river discharge stations and 240 water temperature monitoring stations were used to evaluate the quality of the simulations for Europe and North America. They calculated changes in daily water temperature for the 2040s and 2080s.

The overall projected increase in mean summer (21 June–20 September) water temperatures is 0.7–0.9 (1.4–2.4 ˚C) for the US and 0.8–1.0 (1.4–2.3) ˚C for EU. This implies a summer average

decrease in capacity of power plants of 6.3–19% in Europe and 4.4–16% in the United States depending on cooling system type and climate scenario for 2031–2060. In addition, probabilities of extreme (>90%) reductions in thermoelectric power production will on average increase by a factor of three.

Additional information was provided by Durmayaz and Sogut (2006) who stipulated that the impact of 1˚C increase in temperature of the coolant extracted from environment is predicted to yield a decrease of ~0.45 and ~0.12% in the power output and the thermal efficiency of the pressurized-water reactor nuclear-power plant considered, respectively.

In a report from the European Commission (2011), it is indicated that an increase of 5 (K) of water temperature would decrease nuclear powerplant efficiency by 1%.

Finally, Attia (2015) in a study on the Mediterranean region arrived at the conclusion that an increase of one degree Celsius in temperature of the coolant extracted from environment is forecasted to decrease by 0.444% and 0.152% in the power output and the thermal efficiency of the nuclear-power plant considered.

- **Methodology**

Several equations could be derived from the examples listed above. Durmayaz and Sogut (2006) provide one example, presented in (see Figure 21).

Figure 21 Impact of cooling seawater temperature on thermal efficiency and power output

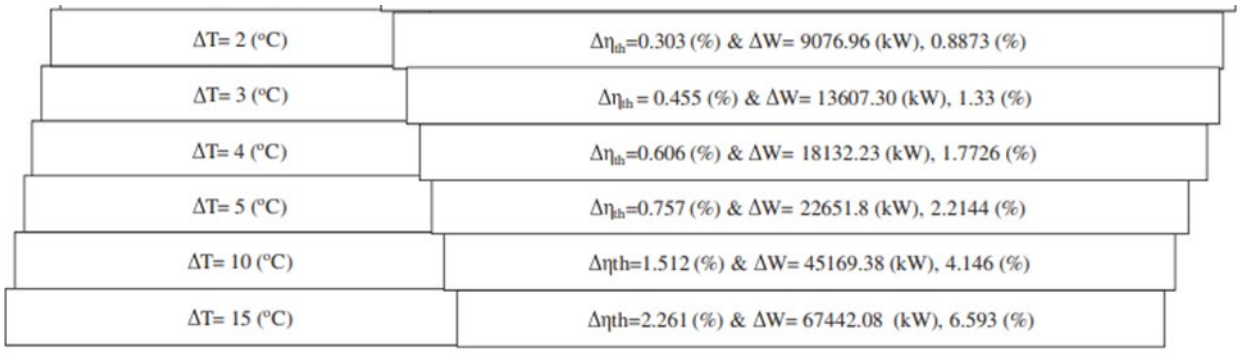

Fig. 8. The impact of cooling seawater temperature, T_{cwi} on the thermal efficiency and output power of the NPP.

Considerations for integration in the CDS toolbox

Water quantity indicators for Europe

2.1.7.2 Air temperature

- **Climate impact**

Ambient temperature is linked with water temperature and hence the cooling system efficiency.

A warmer climate may result in lower thermal efficiency and reduced load—including shutdowns—in thermal power plants.

- **Summary of results**

An increase of 1˚C results in the reduction in efficiency of a nuclear power plant of 0.2425% on average (0.27 (x1 article), 0.1 (x2), and 0.5 (x 1)). We also have an article with two different scenarios for an increase of temperature of 1˚C: When ambient temperature is 0˚C or 20˚C, the impact is of 0.7% and 2.3% decrease in output respectively.

- **Results**

In France, Rousseau (2013) estimated that the average loss in electrical output is 0.32% per increase of one degree in air temperature, with a wide difference between reactors. This average is 0.27% for the 16 median reactors.

In a report from the European Commission (2011) it is stated that for air temperature (cooling towers), an increase in 1(K) air temperature will result in a reduction of 0.1% in efficiency.

In a more general study across Europe, Linnerud et al. (2011) showed that a rise in temperature of 1˚C reduces the supply of nuclear power by about 0.5% through its effect on thermal efficiency. During droughts and heat waves, the production loss may exceed 2.0% ˚C because power plant cooling systems are constrained by physical laws, regulations and access to cooling water.
When the monthly ambient temperature increases with 1˚C, nuclear power plant production is on average reduced with 0.7 percent for temperatures around 0˚C and 2.3 percent for temperatures around 20˚C.

A study led by Lise and van der Laan (2015) provides estimated costs and efficiency changes due to various climate variables. Here are some results displayed in Figure 22 from the article:

Figure 22 – Climate change effect on power generation and investment need for different technologies

Climate change effect	Technology	Lost power generation €/MWh/climate change effect	Investment Need €/kW	Threshold value	Remark
Change in air temperature	Nuclear	0.07	50	5	0.1% less per 1 °C increase
	Biomass	0	150	5	Negligible impact
	Natural gas	0.07	75	5	0.1% efficiency decrease per 1 °C
	Coal	0	100	5	Negligible impact
	Oil	0.07	85	5	0.1% efficiency decrease per 1 °C
	Grids	0.14	40	5	0.2% extra transmission losses per 1 °C
Change in water temperature	Nuclear	0.14	50	5	0.2% per 1 °C increase
	Biomass	0.14	150	5	Small plants have larger cost per unit
	Natural gas	0.14	75	5	Low investment costs
	Coal	0.14	100	5	
	Oil	0.14	85	5	Higher than natural gas

Considerations for integration in the CDS toolbox

- ERA5-Land monthly averaged data from 1981 to present
- ERA5 (present) and CMIP5 (future) 2m air temperature

2.1.8 Geothermal Power

Power plants produce geothermal energy by utilizing geothermal dry steam or geothermal hot water accessed by digging wells. Dry steam or hot water is brought to the surface through pipes and processed into electricity in the power plant.

Dry steam geothermal power plants use steam that is brought from below the earth's surface through pipes, directly to the power plants turbines.

Flash steam geothermal power plants use hot water that is brought from below the earth's surface. The hot water is sprayed into a tank and creates steam.

Binary-cycle geothermal plants use moderate temperature water from a geothermal source and combine it with another chemical to create steam. The steam powers the turbine that drives the generator to create electricity (Kivi, 2017).

2.1.8.1 Air temperature

- **Climate impact**

Higher temperatures have a negative impact on efficiency of the geothermal power plants to cool down the system.

- **Summary of results**

Power output will decrease by about 1% for each 0.56˚C (1˚F) increase in air temperature

- **Results**

In an article published by the US Department of Energy it is indicated that climate change could affect geothermal energy production in the same way that higher temperatures reduce the efficiency of fossil-fuel-boiler electric turbines (Wilbanks, et al., 2008). On the other hand, there is no recent research on other potential impacts in this sector due to climate change. For a typical air-cooled binary cycle geothermal plant with a 330°F resource, power output will decrease about 1% for each 1°F rise in air temperature.

Considerations for integration in the CDS toolbox

ERA5-Land monthly averaged data from 1981 to present

2.1.9 Power Grid Efficiency

The power grid is the network providing electricity from power plants to consumers. This is represented by power lines, alternators, cables, etc.
Weather can have an impact on these infrastructures, resulting in power shutdown or loss of efficiency. When efficiency drops, power plants will have to produce more electricity in order to meet consumer demand.
Climate hazards such as earthquakes, storms, and lightning can create physical damage that will result in a need of replacing or repairing the infrastructure. Climate drivers such as wind, precipitation and mainly temperature, can affect directly the components such as the cables, resulting in loss of efficiency.

2.1.9.1 Temperature

- **Climate risk**

As mentioned above, extreme changes in temperature affect the physical properties of the infrastructures, such as cables, resulting in higher losses.

- **Summary of results**

For transformers, for each 1˚C increase in temperature there is a 1% reduction in efficiency.
For the overall network, for each 1˚C increase there's also a decrease of 1% on output capacity and furthermore, for each supplementary 3˚C increase, for an initial network with 8% initial losses, there's a 1% loss in output.
One study assessed carbon emissions scenarios RCP 2.6, 4.5 and 8.5 impact on transmission capacity that decreases by 1.9-3.9%, 2.2-4.3% and 3.6-5.8% respectively.

- **Results**

In a report made by the European Commission (2011), we learn that the maximum temperature at which the electrical network is bounded is, in general, 80˚C at the conductor surface. Naturally, when the temperature rises, network capacity declines as the resistance of metals increases and the system reaches its maximum operating temperature sooner. The capacity of transformers, for example, can decrease by up to 1% for each 1°C (Kumpulainen, et al., 2007). Similarly, the resistance of copper lines increases by approximately 0.4% for each 1°C. Altogether, network capacity falls by around 1 percent for each for each 1°C of temperature increase. In addition, network losses can increase by 1% if temperature increases by 3°C, in a network with initial losses of 8% (IEA, 2008). Cables sag with higher temperatures, it is said that the extent of sagging depends on the conductor material; the span width and other environmental conditions like wind-speed. For conventional aluminum cables it is approximately 4.5 cm per 1°C rise at the conductor surface with a threshold of 50˚C.

Bartos et al. (2016) present a case study in the US on the ambient temperature effect on electric transmission capacity. They found out that by mid-century (2040–2060), rising air temperatures may reduce summertime transmission capacity by 1.9%–5.8% on average, relative to the 1990–2010 reference period (with the range of impacts being dependent on GCM model and RCP scenario selection).
They also investigated 3 scenarios and stipulated that by mid-century, average transmission capacity reductions range from 1.9%–3.9% under the lowest carbon concentration scenario (RCP 2.6), to 2.2%–4.3% under the medium carbon concentration scenario (RCP 4.5), to 3.6%–5.8% under the highest carbon concentration scenario (RCP 8.5)

On a website section, from Drax, a company specialized in the electricity sector, we can read that when ambient temperatures rise, the ceiling gets lower and their efficiency drops – about 1% for every one degree Celsius gain in temperature. At scale, this can have a significant effect: overall, grids can lose about 1% in efficiency for every three degrees hotter it gets. (Drax, 2017)

2.2 Integration of literature review with the CDS dataset

As indicated in the Introduction, a subset of the indicators and equations presented above have been integrated in the CDS toolbox. We have (i) reviewed the equations to determine their usefulness for SAVi, (ii) assessed what data requirements for each of the equations is available in the Copernicus database, to be accessed via the CDS API (iii) created indicators for climate variables that are relevant for the equations selected, which involves additional processing offline.

The code to download and create the indicators is detailed in Annex I.
The demonstration app in the CDS Toolbox is available at these links:

- Source code: https://cds.climate.copernicus.eu/toolbox-editor/27053/iisd-demo
- App: https://cds.climate.copernicus.eu/apps/27053/iisd-demo

Scientific considerations
In all asset classes we used a systematic approach. We focused on climate variables that are available in two datasets: ERA5 for past reanalysis data (year 1979 to 2019) and CMIP5 for future projections (2006 to 2100, but also including historical simulation from 1979 to 2005). The datasets differ in various ways including model formulation, time-step and available variables. For some variables harmonization was necessary, such as conversion of units of measure, as indicated below. ERA5 is a more detailed dataset, and integrates climate observations, whereas CMIP5 is a coarser dataset specifically intended to test the effect of human activities on the climate, useful for long-term projections but less precise for past and present-days. To make CMIP5 data more useful, were corrected it so that monthly mean over the historical period (1979-2019) matches ERA5. This is a typical operation commonly called bias-correction. The CMIP5 dataset provides climate variables for various models and future climate scenarios. In this work we use four climate models IPSL CM5A MR, BNU ESM, CSIRO MK3 6.0 and MPI ESM MR) and two climate scenarios

(RCP 8.5 for a fossil-fuel intensive, high-emission scenario, and RCP 4.5 for mitigation scenario with CO2 emissions peaking in 2040). We thus have 9 versions of each climate indicator (1 ERA5 and 8 CMIP5). Using different climate models and scenarios is useful to asset the robustness of the results. To perform a full uncertainty analysis, SAVi simulations should be performed for each of the versions, and statistics like mean or range should be calculated on SAVi results, rather than the other way around (we do not recommend using the mean of across models before reading into SAVi). Alternatively, If only one climate scenario should be used, we recommend using RCP 8.5, with IPSL CM5A MR as default climate model. We recommend to always compare with ERA5 simulation, which shall be considered a reference dataset for the past period.

App design considerations
The data is retrieved via the CDS API for all practical purposes, but a demonstration app was also developed for the following indicators: “temperature_2m”, “precipitation”, “runoff”, “evaporation”, “10m_wind_speed”.

2.2.1 Wind technology

Datasets:

- ERA5 monthly data on single level:
  - 10 m wind speed
  - 100 m wind speed (from u and v component)
- CMIP5 monthly data on single level:
  - 10 m wind speed

Indicators created:

- **10 m wind speed:**
  - **Units: m/s**
  - Frequency: monthly
  - Versions: ERA5 and CMIP5
- **100 m wind speed:**
  - **Units: m/s**
  - Frequency: monthly
  - Versions: ERA5 and CMIP5
  - CMIP5 10m wind speed was scaled by 1.65 as first order harmonization with ERA5 100m (see additional information below).

Additional information:
In addition to 10-m wind speed, we use wind speed at 100 m from ERA5, as it represents more accurately the wind experienced by large turbines, unaffected by the boundary layer. For future

projections, we use CMIP5, 10-m wind speed, which we scale to match ERA5 100-m during the period of overlap (1979 to 2019, which resulted in a scaling coefficient of 1.65 for an example location)

Before use, wind data must be corrected to match the appropriate height based on methods listed in the review (Davy, Gnatiuk, Pettersson, & Bobylev, 2018).

2.2.2 Wave technology

See 10-m wind speed and 100-m wind speed above

2.2.3 Solar technology

Datasets:

- ERA5 monthly data on single level:
  - 'mean_surface_downward_short_wave_radiation_flux'
    - Note: another variable 'surface_solar_radiation_downwards' was also available but expressed in J/m2 (cumulative) that is why we opted for the above variable as we prefer mean flux W/m2
  - “2-m air temperature”
  - “10-m wind speed”
- CMIP5 monthly data on single level:
  - 'surface_solar_radiation_downwards'
  - “2-m air temperature”
  - “10-m wind speed”

Indicator created:

- **Solar radiation**:
  - Units: W/m2
  - Frequency: monthly
  - ERA5 and CMIP5 versions
  - Note this variable already integrates cloud cover, so we do not provide the cloud cover variable here.
- **Air temperature**:
  - Units: degrees Celsius
  - Frequency: monthly
  - Versions: ERA5 and CMIP5
  - Note: converted from Kelvin to degrees Celsius
- **10 m wind speed:**
  - **Units: m/s**
  - Frequency: monthly

- Versions: ERA5 and CMIP5
- **Not yet implemented**

Additional information

Dust and ashes data were not considered specifically, though they should be accounted for in "solar radiation" indicator as CMIP5 models typically include a component for dust and volcano eruption (the latter only in the historical period).

2.2.4 Hydropower

Datasets:

- ERA5 monthly data on single level: "Mean total precipitation rate"
- CMIP5 monthly data on single level: "Mean precipitation flux"

Indicators created:

- **Precipitation**:
  - Units: mm per month
  - Frequency: monthly

Additional information

Precipitation changes shall be used here as proxy for river discharge changes in hydropower equations. We decided to use precipitation data instead of specific products for river discharge estimation because this is the only variable that is available 1) globally and 2) for past and future. In particular, we decided against the following datasets:

- "River discharge and related historical data from the Global Flood Awareness System": available globally but only until present.
- "Water quantity indicators for Europe": available for future but only in Europe.

More detailed information about precipitation variable in ERA5/CMIP5 can be found in the road asset ("road runoff").

2.2.5 Gas power

Datasets:

- ERA5 monthly data on single level:
  - "2-m air temperature"
  - "2m dewpoint temperature"
- CMIP5 monthly data on single level:
  - "2-m air temperature"
  - "near_surface_relative_humidity"

Indicators created:

- **Air temperature**:
  - Units: degrees Celsius
  - Frequency: monthly
  - Versions: ERA5 and CMIP5
  - Note: converted from Kelvin to degrees Celsius

- **Relative humidity**
  - Units: %
  - Frequency: monthly
  - Versions: ERA5 and CMIP5
  - Method: available out-of-the-box for CMIP5, not for ERA5. For ERA5, we calculated relative humidity from 2-m temperature T and 2-m dewpoint temperature TD (both in degrees Celsius) with the thermodynamic formula
    - 100*(exp((17.625*TD)/(243.04+TD))/exp((17.625*T)/(243.04+T)))

2.2.6 Coal power

Datasets:

- Same as for gas power generation

Indicator created:

- **Air temperature**
  - Same as for gas power generation
- **Relative humidity**
  - Same as for gas power generation

2.2.7 Nuclear power

Datasets:

- ERA5 monthly data on single level:
  - “2-m air temperature”
  - “Mean total precipitation rate”
- CMIP5 monthly data on single level:
  - “2-m air temperature”
  - “Mean precipitation flux“

Indicators created:

- **Air temperature**:

- Units: degrees Celsius
- Frequency: monthly
- Versions: ERA5 and CMIP5
- Note: converted from Kelvin to degrees Celsius

- **Precipitation**:
  - Units: mm per month
  - Frequency: monthly

Additional information

Some equations investigated in this section take river temperature as input. However, river temperature was not available as global datasets, as far as we could tell. In particular, we decided not to use the following dataset:

- "Water quality indicators for European rivers": only available for Europe

As a result, we suggest that river temperature can be derived from air temperature and precipitation. Additional research must be done to find a useful model formulation.

One indicator in the literature review was based on sea water temperature (for plants using sea water as cooling source). As none of the use cases are located at the sea, nor relate to such plant, we did not include sea surface temperature as climate indicator here.

2.2.8 Geothermal power

Datasets:

- ERA5 monthly data on single level: "2-m air temperature"
- CMIP5 monthly data on single level: "2-m air temperature"

Indicators created:

- **Air temperature**:
  - Units: degrees Celsius
  - Frequency: monthly
  - Versions: ERA5 and CMIP5
  - Note: converted from Kelvin to degrees Celsius

2.3 Integration of climate indicators into the SAVi energy model

Figure 23 presents the CLD for the SAVi Energy model. Climate-related variables and parameters developed for and extracted from the CDS toolbox are illustrated in pink. Energy-related climate indicators developed in the CDS toolbox include impacts on the efficiency of thermal and renewable power generation assets as well as temperature-related impacts on grid efficiency.

Figure 23 Causal Loop Diagram for the energy sector - CDS variables included

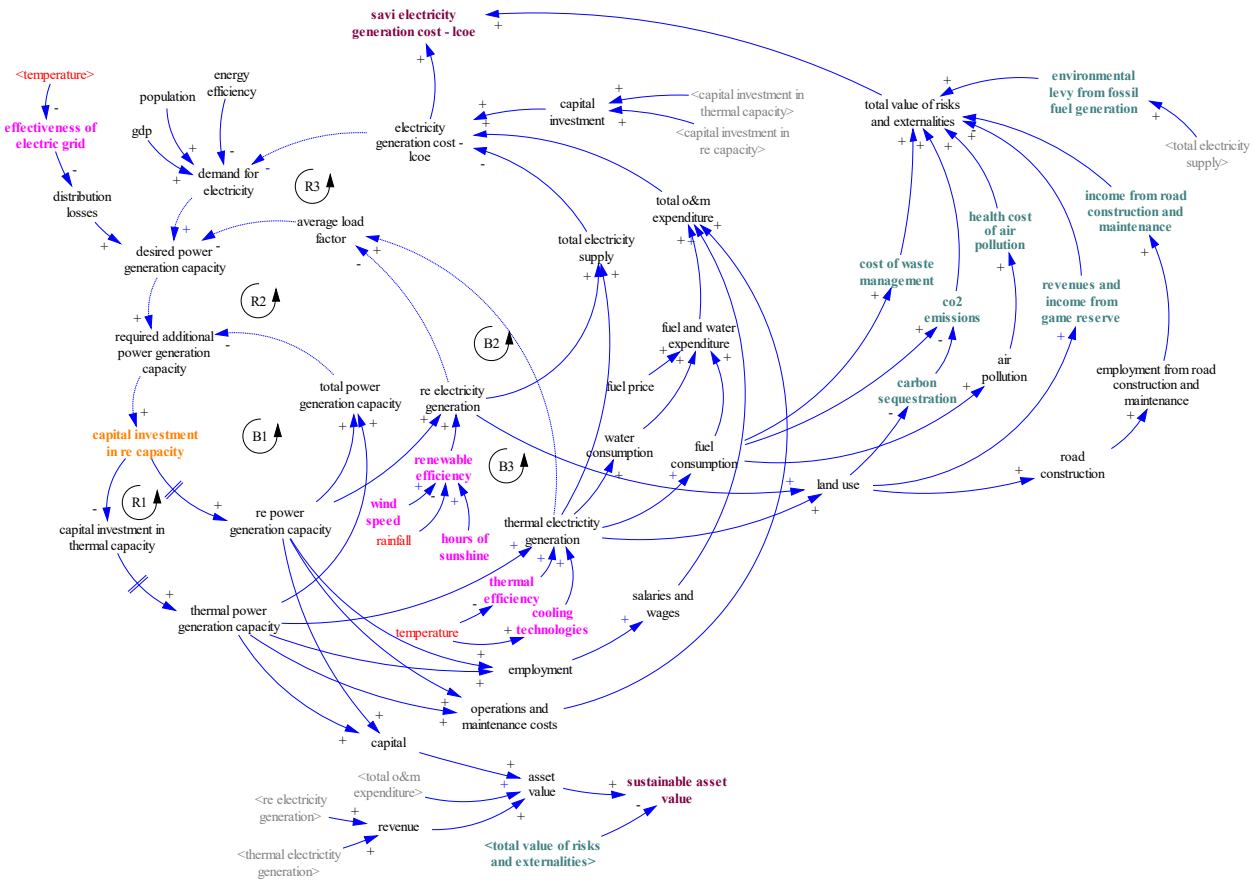

The impact of climate variables on power generation efficiency vary between thermal and renewable power plants. Thermal efficiency is reflected in the load factor of generation assets and determines the electricity yield given the amount of inputs (fossil fuels) used, technological specifications of the plant and location. The thermal efficiency indicator is calculated based on outside temperature and affects electricity generation output, based on the extent to which an asset is affected by outside temperatures. In the case of coal, gas, and nuclear, reductions in generation efficiency were observed as outside temperatures increased. In addition to fossil fuel generation, the efficiency of biomass technologies is also affected by temperature, using heat-based technologies.

Renewable power generation potential depends on the availability of 'inputs' required for renewable power generation. Climate impacts on renewable generation are technology specific. Inputs for calculating this indicator include for example solar radiation, cloud cover and wind speed.

Grid efficiency indicates the amount of electricity that is lost throughout the transmission process, commonly referred to as 'transmission losses'. With increases in mean air temperature, the efficiency of the electricity grid declines. The grid effectiveness indicator developed for and extracted from the CDS provides information about current and future grid effectiveness, given

changes in temperature. The projections forecast grid-related transmission losses, which, in combination with impacts on generation efficiency and electricity demand, yields gross generation required. This can contribute to supporting the development of energy strategies and power generation projects.

2.4 Behavioral impacts resulting from the integration of climate variables

Power generation efficiency indicators developed for and obtained from the CDS toolbox cause seasonal fluctuations in electricity generation and transmission efficiency. Using these CDS indicators allows us to assess economic and environmental consequences emerging from changes in generation efficiency.

A reduction in thermal generation efficiency leads to higher fuel use and hence higher generation cost. In case of a reduction in plant output, either total generation will decrease and generation will be lower, or the asset owners are forced to implement site-specific measures to maintain generation at the same level, or expand capacity.

The efficiency of renewable generation uses climate data to forecast generation efficiency and hence indicates seasonal changes in power output of renewable generation assets. As a consequence, this indicator supports the site-specific feasibility assessment of different renewable generation technologies (e.g. revenue generation changes with seasons, affecting the potential cash flow and debt repayment). Specifically, since renewable energy sources (excluding biomass) do not rely on fuel inputs and have primarily fixed costs, the profitability of the asset is more predominantly affected by the fluctuations in generation. In other words, if generation declines, electricity sales decline as well and cause the return on investment to be lower compared to a no-climate scenario.

2.5 Simulation results

The results presented in this section consider seven different technologies with an annual generation of 4.89 million MWh in the context of Johannesburg, South Africa. Information concerning technology types and their baseline load factor are provided in Table 2. This analysis assumes that all technologies are established in 2020 and produce electricity between 2022 and 2100[5].

	Coal	Gas	Nuclear	Biomass	Hydro	Solar	Wind
Capacity	630.0	1,116.9	620.5	797.8	1,329.6	2,252.7	1,583.8
Load factor	88.6%	50.0%	90.0%	70.0%	56.4%	24.8%	35.3%

[5] Capacity lifetime varies by technology, which indicates that reinvestments would be required to maintain the installed capacity level over 80 years. The presented simulation serves for illustration purposes and does not reconsider reinvestment in capacity.

Table 2: Installed capacity and load factor

Three CDS-based impacts were integrated into the SAVi Energy model: (1) climate impacts on load factor, (2) effect of temperature on thermal efficiency, and (3) effect of temperature on transmission line efficiency.

2.5.1 Climate impacts on load factor

Weather conditions and changes therein affect the degree to which capacity can be utilized to produce electricity. Furthermore, different technologies are impacted by different climate variables and to a different extent. While thermal generators depend on cold water for cooling purposes, the load factor of renewables depends on the availability of the respective input to the energy production process (e.g. water, wind speed, solar radiation) and impacts related to technological constraints (e.g. impact of temperature on the efficiency of solar panels).

The equations used for the integration of climate impacts on the load factor of the different technologies are listed in Table 3.

Technology	**Equation**	**Reference**
Coal Gas Nuclear Biomass	IF THEN ELSE (seasonal temperature > THRESHOLD TEMPERATURE FOR THE OPERATION OF POWER PLANTS, ((2/52) + (2/52) * (temperature relative to threshold - 1) ^ ELASTICITY OF LOAD FACTOR FOR EXCEEDING THE THRESHOLD LIMIT) ,1)	Based on (U.S. DoE, 2013)
Hydro	Mean annual precipitation$_{t+n}$ / Mean annual precipitation$_{t0}$	Based on (Wilbanks, et al., 2008)
Solar	1 - IF THEN ELSE (Mean annual temperature > Temperature threshold for optimal functioning, (Mean annual temperature - Temperature threshold for optimal functioning) * 0.01, 0)	Based on (Panagea, Tsanis, Koutroulis, & Grillakis, 2014)
Wind	Effect of relative wind speed on load factor(Monthly wind speed$_{tn}$ / Mean monthly wind speed$_{t1-5}$)	Based on (Harrison & Wallace, 2005)

Table 3: Climate impacts on load factor by generation technology

Table 4 presents the average load factor and climate impacts for the context of Johannesburg for each decade between 2020 and 2100 by technology[6].

[6] The temperature thresholds for thermal generation and solar power were artificially reduced to show impacts in the context of Johannesburg. The threshold for thermal power plants was reduced from 35°C to 27°C and the threshold for solar power from 25°C to 15°C.

Load factor by technology	2020-2030	2030-2040	2040-2050	2050-2060	2060-2070	2070-2080	2080-2090	2090-2100
Coal								
Initial load factor	88.64%	88.64%	88.64%	88.64%	88.64%	88.64%	88.64%	88.64%
Climate impacts on load factor	0.00%	0.00%	0.00%	-0.68%	-2.05%	-9.56%	-12.97%	-27.99%
Real load factor	88.64%	88.64%	88.64%	87.96%	86.59%	79.08%	75.67%	60.65%
Gas								
Initial load factor	50.00%	50.00%	50.00%	50.00%	50.00%	50.00%	50.00%	50.00%
Climate impacts on load factor	0.00%	0.00%	0.00%	-0.39%	-1.16%	-5.39%	-7.32%	-15.79%
Real load factor	50.00%	50.00%	50.00%	49.61%	48.84%	44.61%	42.68%	34.21%
Nuclear								
Initial load factor	90.00%	90.00%	90.00%	90.00%	90.00%	90.00%	90.00%	90.00%
Climate impacts on load factor	0.00%	0.00%	0.00%	-0.69%	-2.08%	-9.71%	-13.17%	-28.42%
Real load factor	90.00%	90.00%	90.00%	89.31%	87.92%	80.29%	76.83%	61.58%
Hydropower								
Initial load factor	56.35%	56.35%	56.35%	56.35%	56.35%	56.35%	56.35%	56.35%
Historical weather impacts on load factor	14.35%	14.35%	14.35%	14.35%	14.35%	14.35%	14.35%	14.35%
Climate impacts on load factor	-1.21%	-0.56%	-4.23%	-2.97%	-2.69%	-4.03%	-5.36%	-8.00%
Real load factor	40.79%	41.44%	37.77%	39.03%	39.31%	37.97%	36.64%	34.00%
Solar								
Initial load factor	24.79%	24.79%	24.79%	24.79%	24.79%	24.79%	24.79%	24.79%
Climate impacts on load factor	-0.80%	-0.91%	-1.13%	-1.23%	-1.29%	-1.58%	-1.73%	-1.95%
Real load factor	23.99%	23.88%	23.66%	23.56%	23.50%	23.21%	23.06%	22.84%
Wind								
Initial load factor	35.26%	35.26%	35.26%	35.26%	35.26%	35.26%	35.26%	35.26%
Climate impacts on load factor	2.41%	3.22%	3.40%	3.14%	3.89%	4.34%	4.00%	4.53%
Real load factor	37.67%	38.48%	38.66%	38.40%	39.15%	39.60%	39.26%	39.79%

Table 4: Load factor and climate impacts by technology

The results indicate significant reductions in the load factor for thermal producers. For illustration purposes, the temperature threshold for potential shutdowns was set to 25°C. With a projected maximum annual temperature in Johannesburg is 30°C (Climate scenario: IPSL RCP8.5), impacts on thermal generation are forecasted to start occurring between 2050 and 2060, and increase in severity until 2100.

For renewable capacity, the results indicate a decline in load factor for hydropower and solar generation, while wind shows an increase in the load factor for wind power. In the case of hydropower, the decline in load factor is caused by the forecasted decline in precipitation for

Johannesburg. Lower precipitation reduces water availability for hydropower generation and consequently reduces the potential for hydropower-based electricity generation. For solar powered generation, impacts are throughout the simulation, with an absolute decline of 1.15% by 2100 compared to 2020. This is because the seasonal temperature exceeds the temperature threshold for optimal functioning until the last decade (2090-2100). Wind powered generation benefits from higher wind speeds in the future, which increase the load factor on average by 4.5% by 2100.

2.5.1.1 Economic implications of load factor impacts

Table 5 presents the integrated CBA assessing the economic consequences of climate-related impacts on the load factor. The reduction in load factor has implications for the amount of electricity that can be produced with each technology, which translates into direct impacts on revenues and profits.

Between 2020 and 2100, a net reduction between 5.15% and 8.54% in cumulative revenues is observed for all technologies as a consequence of lower capacity utilization. The only exception is onshore wind for which results indicate an increase of 9.88% in cumulative revenues.

Technology	Coal			Gas			Nuclear			Biomass		
Scenario	Climate impacts	No climate impacts	*Impacts vs no impacts*	Climate impacts	No climate impacts	*Impacts vs no impacts*	Climate impacts	No climate impacts	*Impacts vs no impacts*	Climate impacts	No climate impacts	*Impacts vs no impacts*
Investment and cost												
Capital Cost	17.5	17.5	*0.0%*	11.3	11.3	*0.0%*	36.6	36.6	*0.0%*	24.6	24.6	*0.0%*
O&M Cost	42.5	42.5	*0.0%*	25.5	25.5	*0.0%*	99.2	99.2	*0.0%*	64.1	64.1	*0.0%*
Fuel Cost	94.4	102.3	*-7.7%*	201.4	218.4	*-7.7%*	0.0	0.0	*0.0%*	7.6	7.6	*0.0%*
Transitional Risk												
Carbon Tax	51.7	56.0	*-7.7%*	13.0	14.1	*-7.7%*	0.0	0.0	*0.0%*	0.0	0.0	*0.0%*
(1) Total costs	**206.1**	**218.4**	***-5.6%***	**251.3**	**269.3**	***-6.7%***	**135.8**	**135.8**	***0.0%***	**96.2**	**96.2**	***0.0%***
Externalities												
Social Cost of Carbon	196.85	213.36	*-7.7%*	49.96	54.12	*-7.7%*	0.27	0.27	*0.0%*	0.31	0.31	*0.0%*
Wastewater treatment cost	6.73	7.29	*-7.7%*	14.20	15.40	*-7.7%*	37.38	40.52	*-7.7%*	22.43	24.31	*-7.7%*
Cost of ash disposal	48.66	52.74	*-7.7%*	0.00	0.00	*0.0%*	0.00	0.00	*0.0%*	0.00	0.00	*0.0%*
Health cost of air pollution	3.29	3.29	*0.0%*	1.58	1.58	*0.0%*	0.03	0.03	*0.0%*	5.24	5.24	*0.0%*
(2) Total externalities	**255.5**	**276.7**	***-7.7%***	**65.7**	**71.1**	***-7.5%***	**37.7**	**40.8**	***-7.7%***	**28.0**	**29.9**	***-6.3%***
(1) + (2) Total cost and externalities	**513.3**	**551.1**	***-6.9%***	**330.1**	**354.6**	***-6.9%***	**173.5**	**176.6**	***-1.8%***	**124.2**	**126.1**	***-1.5%***
(3) Revenues from electricity generation	283.5	307.3	*-7.7%*	283.5	307.3	*-7.7%*	283.5	307.3	*-7.7%*	283.5	307.3	*-7.7%*
(1) - (3) Cost minus revenues	**-77.34**	**-88.88**	***-13.0%***	**-32.12**	**-37.92**	***-15.3%***	**-147.63**	**-171.44**	***-13.9%***	**-187.23**	**-211.04**	***-11.3%***
(1) + (2) - (3) Net societal cost of power generation	**229.9**	**243.8**	***-5.7%***	**46.6**	**47.3**	***-1.4%***	**-110.0**	**-130.6**	***-15.8%***	**-159.3**	**-181.2**	***-12.1%***

Table 5: Integrated cost benefit analysis impact on load factor in billion ZAR – Thermal generators

Technology	Hydropower			Solar			Wind (onshore)		
Scenario	Climate impacts	No climate impacts	*Impacts vs no impacts*	Climate impacts	No climate impacts	*Impacts vs no impacts*	Climate impacts	No climate impacts	*Impacts vs no impacts*
Investment and cost									
Capital Cost	21.0	21.0	*0.0%*	35.2	35.2	*0.0%*	26.7	26.7	*0.0%*
O&M Cost	30.4	30.4	*0.0%*	27.0	27.0	*0.0%*	54.8	54.8	*0.0%*
Fuel Cost	0.0	0.0	*0.0%*	0.0	0.0	*0.0%*	0.0	0.0	*0.0%*
Transitional Risk									
Carbon Tax	0.0	0.0	*0.0%*	0.0	0.0	*0.0%*	0.0	0.0	*0.0%*
(1) Total costs	**51.3**	**51.3**	***0.0%***	**62.2**	**62.2**	***0.0%***	**81.5**	**81.5**	***0.0%***
Externalities									
Social Cost of Carbon	0.21	0.21	*0.0%*	0.52	0.52	*0.0%*	0.51	0.51	*0.0%*
Wastewater treatment cost	0.00	0.00	*0.0%*	0.00	0.00	*0.0%*	0.00	0.00	*0.0%*
Cost of ash disposal	0.00	0.00	*0.0%*	0.00	0.00	*0.0%*	0.00	0.00	*0.0%*
Health cost of air pollution	0.00	0.00	*0.0%*	0.00	0.00	*0.0%*	0.00	0.00	*0.0%*
(2) Total externalities	**0.2**	**0.2**	***0.0%***	**0.5**	**0.5**	***0.0%***	**0.5**	**0.5**	***0.0%***
(1) + (2) Total cost and externalities	**51.6**	**51.6**	***0.0%***	**62.8**	**62.8**	***0.0%***	**82.0**	**82.0**	***0.0%***
(3) Revenues from electricity generation	279.9	307.3	*-8.9%*	290.6	307.3	*-5.4%*	338.9	307.3	*10.3%*
(1) - (3) Cost minus revenues	**-228.59**	**-255.92**	***-10.7%***	**-228.35**	**-245.03**	***-6.8%***	**-257.39**	**-225.76**	***14.0%***
(1) + (2) - (3) Net societal cost of power generation	**-228.4**	**-255.7**	***-10.7%***	**-227.8**	**-244.5**	***-6.8%***	**-256.9**	**-225.3**	***14.0%***

Table 5 continued: Integrated cost benefit analysis impact on load factor in billion ZAR – Renewable generators

2.5.2 Climate impacts on thermal efficiency

Studies suggest that, as temperatures rise, the conversion efficiency of thermal power plants will decline. For this assessment, we assume that generators can maintain the same level of output, however need to use additional fuel to maintain the desired generation.

Temperature impacts on power generation efficiency only apply to thermal generators and are related to the optimal operation conditions determined by the respective technology. The equations used for each thermal technology are presented in Table 6.

Technology	Equation	Reference
Coal	Impact = 1-IF THEN ELSE (Tair>Threshold for optimal functioning, (Tair-Threshold for optimal functioning)*0.038, 0)	Based on (Bhattacharya & Sengupta, 2016)
Gas	Impact = 1 - ((T - 2.76) * 0.21)/100	Based on (Maulbetsch & Di Filippo, 2006)
Nuclear	Impact = 1-IF THEN ELSE (Tair>Threshold for optimal functioning, (Tair-Threshold for optimal functioning)*0.005, 0)	Based on (U.S. DoE, 2013)

Table 6: Climate impacts on thermal efficiency by generation technology

Based on the above, climate change related impacts on thermal efficiency causes producers to use more fuel, and hence incur higher costs, compared to the no climate scenario. The projected fuel use for coal and gas power generation is indicated in Figure 24 for illustration purposes.

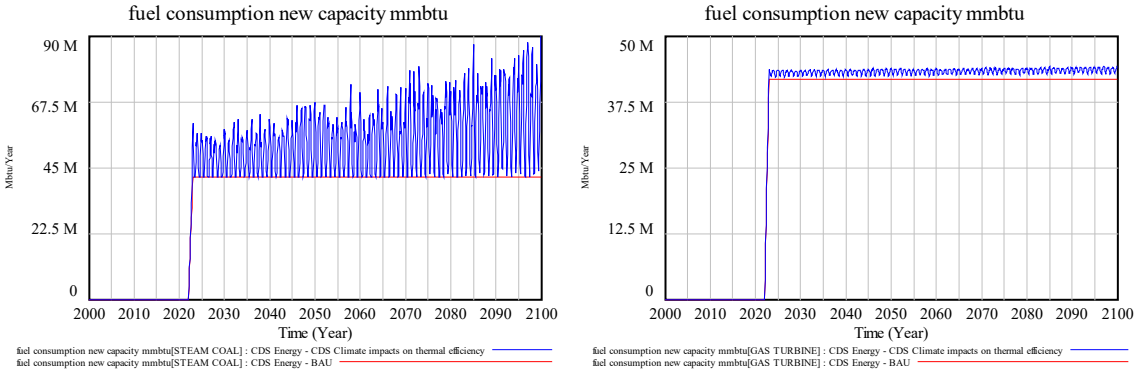

Figure 24: Fuel use for coal and gas powered generation with and without climate impacts

The reduction in efficiency causes thermal producers to incur higher average fuel costs with each decade. The impacts on the fuel expenditure for coal and gas powered power plants are presented in Table 7.

Technology	2022-2030	2030-2040	2040-2050	2050-2060	2060-2070	2070-2080	2080-2090	2090-2100
Coal	15.5%	18.1%	23.8%	26.4%	28.1%	37.5%	42.0%	50.7%
Gas	3.1%	3.2%	3.4%	3.6%	3.7%	4.0%	4.2%	4.4%

Table 7: Fuel use CDS climate impact scenario relative to the no climate impacts scenario

2.5.2.1 Economic implications of thermal efficiency impacts

The integrated CBA for the impacts on thermal efficiency is presented in Table 8. Climate impacts on thermal efficiency are reflected in higher fuel costs for fossil-fuel based producers. Consequently, all externalities related to fuel use such as social cost of carbon or the cost of fly ash disposal increase proportionally with the use of fuel. As the tables show, there are no impacts on renewable power generation. Compared to the no impact scenario, there are no changes in capital cost or power generation related externalities.

Technology	Coal			Gas			Nuclear			Biomass		
Scenario	Climate impacts	No climate impacts	*Impacts vs no impacts*	Climate impacts	No climate impacts	*Impacts vs no impacts*	Climate impacts	No climate impacts	*Impacts vs no impacts*	Climate impacts	No climate impacts	*Impacts vs no impacts*
Investment and cost												
Capital Cost	17.5	17.5	*0.0%*	11.3	11.3	*0.0%*	36.6	36.6	*0.0%*	24.6	24.6	*0.0%*
O&M Cost	42.5	42.5	*0.0%*	25.5	25.5	*0.0%*	99.2	99.2	*0.0%*	64.1	64.1	*0.0%*
Fuel Cost	133.9	102.3	*30.9%*	226.5	218.4	*3.7%*	0.0	0.0	*0.0%*	7.6	7.6	*0.0%*
Transitional Risk												
Carbon Tax	73.3	56.0	*30.9%*	14.6	14.1	*3.7%*	0.0	0.0	*0.0%*	0.0	0.0	*0.0%*
(1) Total costs	**267.3**	**218.4**	***22.4%***	**278.0**	**269.3**	***3.2%***	**135.8**	**135.8**	***0.0%***	**96.2**	**96.2**	***0.0%***
Externalities												
Social Cost of Carbon	279.13	213.36	*30.8%*	56.12	54.12	*3.7%*	0.27	0.27	*0.0%*	0.31	0.31	*0.0%*
Wastewater treatment cost	9.54	7.29	*30.9%*	15.97	15.40	*3.7%*	41.67	40.52	*2.8%*	24.31	24.31	*0.0%*
Cost of ash disposal	69.02	52.74	*30.9%*	0.00	0.00	*0.0%*	0.00	0.00	*0.0%*	0.00	0.00	*0.0%*
Health cost of air pollution	4.31	3.29	*30.9%*	1.64	1.58	*3.7%*	0.03	0.03	*2.8%*	5.24	5.24	*0.0%*
(2) Total externalities	**362.0**	**276.7**	***30.8%***	**73.7**	**71.1**	***3.7%***	**42.0**	**40.8**	***2.8%***	**29.9**	**29.9**	***0.0%***
(1) + (2) Total cost and externalities	**702.6**	**551.1**	***27.5%***	**366.4**	**354.6**	***3.3%***	**177.8**	**176.6**	***0.6%***	**126.1**	**126.1**	***0.0%***
(3) Revenues from electricity generation	307.3	307.3	*0.0%*	307.3	307.3	*0.0%*	307.3	307.3	*0.0%*	307.3	307.3	*0.0%*
(1) - (3) Cost minus revenues	**-40.01**	**-88.88**	***-55.0%***	**-29.24**	**-37.92**	***-22.9%***	**-171.44**	**-171.44**	***0.0%***	**-211.04**	**-211.04**	***0.0%***
(1) + (2) - (3) Net societal cost of power generation	**395.3**	**243.8**	***62.1%***	**59.1**	**47.3**	***25.0%***	**-129.5**	**-130.6**	***-0.9%***	**-181.2**	**-181.2**	***0.0%***

Table 8: Integrated CBA for climate impacts on thermal efficiency in billion ZAR

Technology	Hydropower			Solar			Wind (onshore)		
Scenario	Climate impacts	No climate impacts	*Impacts vs no impacts*	Climate impacts	No climate impacts	*Impacts vs no impacts*	Climate impacts	No climate impacts	*Impacts vs no impacts*
Investment and cost									
Capital Cost	21.0	21.0	0.0%	35.2	35.2	0.0%	26.7	26.7	0.0%
O&M Cost	30.4	30.4	0.0%	27.0	27.0	0.0%	54.8	54.8	0.0%
Fuel Cost	0.0	0.0	0.0%	0.0	0.0	0.0%	0.0	0.0	0.0%
Transitional Risk									
Carbon Tax	0.0	0.0	0.0%	0.0	0.0	0.0%	0.0	0.0	0.0%
(1) Total costs	**51.3**	**51.3**	**0.0%**	**62.2**	**62.2**	**0.0%**	**81.5**	**81.5**	**0.0%**
Externalities									
Social Cost of Carbon	0.00	0.00	0.0%	0.52	0.52	0.0%	0.51	0.51	0.0%
Wastewater treatment cost	0.00	0.00	0.0%	0.00	0.00	0.0%	0.00	0.00	0.0%
Cost of ash disposal	0.00	0.00	0.0%	0.00	0.00	0.0%	0.00	0.00	0.0%
Health cost of air pollution	0.00	0.00	0.0%	0.00	0.00	0.0%	0.00	0.00	0.0%
(2) Total externalities	**0.0**	**0.0**	**0.0%**	**0.5**	**0.5**	**0.0%**	**0.5**	**0.5**	**0.0%**
(1) + (2) Total cost and externalities	**51.3**	**51.3**	**0.0%**	**62.8**	**62.8**	**0.0%**	**82.0**	**82.0**	**0.0%**
(3) Revenues from electricity generation	307.3	307.3	0.0%	307.3	307.3	0.0%	307.3	307.3	0.0%
(1) - (3) Cost minus revenues	**-255.92**	**-255.92**	**0.0%**	**-245.03**	**-245.03**	**0.0%**	**-225.76**	**-225.76**	**0.0%**
(1) + (2) - (3) Net societal cost of power generation	**-255.9**	**-255.9**	**0.0%**	**-244.5**	**-244.5**	**0.0%**	**-225.3**	**-225.3**	**0.0%**

Table 8 continued: Integrated CBA for climate impacts on thermal efficiency in billion ZAR

2.5.3 Climate impacts on transmission lines

The conductivity of transmission lines is affected by the surrounding air temperature and decreases as summer air temperatures increase (U.S. DoE, 2013). As a consequence of reduced transmission efficiency, not all the electricity produced can be sold on the market. The impacts of transmission lines in the SAVi model are assumed to affect the revenues of power producers.

According to the International Energy Agency (2008), a network with initial losses of 8% will see a 1% reduction in transmission efficiency for each 1°C increase in temperature relative to a reference temperature. This is equivalent to a 12.5% increase in grid losses per degree Celsius in additional air temperature. The formulation used for the climate impacts assumes a grid loss factor of 15%, and hence an increase in losses of 0.63% per 1°C (12.5% out of 15%). The following equation is used to determine the impacts of temperature changes in grid efficiency:

*Temperature impacts on grid efficiency = 1 - IF THEN ELSE (Tair>Treference, (Tair-Treference) * 0.0063, 0)*

The impacts are hence dependent on whether air temperature exceeds the reference temperature for the initial losses.

The reduction in revenues is affected by the seasonality of temperature, as illustrated in Figure 25. Since the generation of all assets is assumed equal in this assessment, revenues generated by coal power plants serves for illustration purposes.

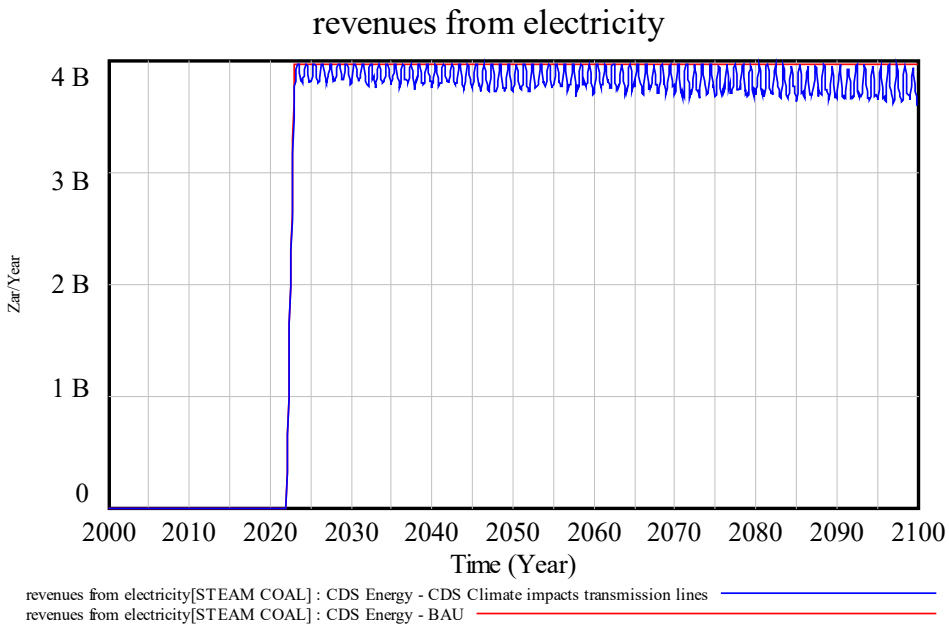

Figure 25: Impacts of grid efficiency on revenues from power generation

For all producers, revenue generation in the no climate scenario averages ZAR 3.94 billion per year between 2022 and 2100. In the scenario including CDS climate impacts, average annual revenues are projected at ZAR 3.81 billion, which is 3.4% lower compared to the no climate

scenario. Cumulatively, the losses incurred from reduced grid efficiency total ZAR 10.42 billion between 2022 and 2100, which is equivalent to annual foregone revenues of ZAR 134 million per year on average.

2.5.3.1 Economic implications of grid efficiency impacts

The forecasted impacts of changes in grid efficiency on revenues from power generation between the no climate and climate impact scenarios is presented in Table 9. Aside from revenue generation, the changes in forecasted grid efficiency do not affect the operational costs of the power plants. Consequently, this effect changes the revenues from generators, which in turn affects profitability and the total societal cost of power generation.

Technology	Coal			Gas			Nuclear			Biomass		
Scenario	Climate impacts	No climate impacts	*Impacts vs no impacts*	Climate impacts	No climate impacts	*Impacts vs no impacts*	Climate impacts	No climate impacts	*Impacts vs no impacts*	Climate impacts	No climate impacts	*Impacts vs no impacts*
Investment and cost												
Capital Cost	17.5	17.5	*0.0%*	11.3	11.3	*0.0%*	36.6	36.6	*0.0%*	24.6	24.6	*0.0%*
O&M Cost	42.5	42.5	*0.0%*	25.5	25.5	*0.0%*	99.2	99.2	*0.0%*	64.1	64.1	*0.0%*
Fuel Cost	102.3	102.3	*0.0%*	218.4	218.4	*0.0%*	0.0	0.0	*0.0%*	0.0	0.0	*0.0%*
Transitional Risk												
Carbon Tax	56.0	56.0	*0.0%*	14.1	14.1	*0.0%*	0.0	0.0	*0.0%*	0.0	0.0	*0.0%*
(1) Total costs	**218.4**	**218.4**	***0.0%***	**269.3**	**269.3**	***0.0%***	**135.8**	**135.8**	***0.0%***	**88.6**	**88.6**	***0.0%***
Externalities												
Social Cost of Carbon	213.36	213.36	*0.0%*	54.12	54.12	*0.0%*	0.27	0.27	*0.0%*	0.31	0.31	*0.0%*
Wastewater treatment cost	7.29	7.29	*0.0%*	15.40	15.40	*0.0%*	40.52	40.52	*0.0%*	24.31	24.31	*0.0%*
Cost of ash disposal	52.74	52.74	*0.0%*	0.00	0.00	*0.0%*	0.00	0.00	*0.0%*	0.00	0.00	*0.0%*
Health cost of air pollution	3.29	3.29	*0.0%*	1.58	1.58	*0.0%*	0.03	0.03	*0.0%*	5.24	5.24	*0.0%*
(2) Total externalities	**276.7**	**276.7**	***0.0%***	**71.1**	**71.1**	***0.0%***	**40.8**	**40.8**	***0.0%***	**29.9**	**29.9**	***0.0%***
(1) + (2) Total cost and externalities	**551.1**	**551.1**	***0.0%***	**354.6**	**354.6**	***0.0%***	**176.6**	**176.6**	***0.0%***	**118.5**	**118.5**	***0.0%***
(3) Revenues from electricity generation	296.8	307.3	*-3.4%*	296.8	307.3	*-3.4%*	296.8	307.3	*-3.4%*	296.8	307.3	*-3.4%*
(1) - (3) Cost minus revenues	**-78.46**	**-88.88**	***-11.7%***	**-27.50**	**-37.92**	***-27.5%***	**-161.02**	**-171.44**	***-6.1%***	**-208.20**	**-218.63**	***-4.8%***
(1) + (2) - (3) Net societal cost of power generation	**254.3**	**243.8**	***4.3%***	**57.7**	**47.3**	***22.0%***	**-120.2**	**-130.6**	***-8.0%***	**-178.3**	**-188.8**	***-5.5%***

Table 9: Integrated CBA for climate impacts on transmission lines

Technology	Hydropower			Solar			Wind (onshore)		
Scenario	Climate impacts	No climate impacts	*Impacts vs no impacts*	Climate impacts	No climate impacts	*Impacts vs no impacts*	Climate impacts	No climate impacts	*Impacts vs no impacts*
Investment and cost									
Capital Cost	21.0	21.0	*0.0%*	35.2	35.2	*0.0%*	26.7	26.7	*0.0%*
O&M Cost	30.4	30.4	*0.0%*	27.0	27.0	*0.0%*	54.8	54.8	*0.0%*
Fuel Cost	0.0	0.0	*0.0%*	0.0	0.0	*0.0%*	0.0	0.0	*0.0%*
Transitional Risk									
Carbon Tax	0.0	0.0	*0.0%*	0.0	0.0	*0.0%*	0.0	0.0	*0.0%*
(1) Total costs	**51.3**	**51.3**	***0.0%***	**62.2**	**62.2**	***0.0%***	**81.5**	**81.5**	***0.0%***
Externalities									
Social Cost of Carbon	0.00	0.00	*0.0%*	0.52	0.52	*0.0%*	0.51	0.51	*0.0%*
Wastewater treatment cost	0.00	0.00	*0.0%*	0.00	0.00	*0.0%*	0.00	0.00	*0.0%*
Cost of ash disposal	0.00	0.00	*0.0%*	0.00	0.00	*0.0%*	0.00	0.00	*0.0%*
Health cost of air pollution	0.00	0.00	*0.0%*	0.00	0.00	*0.0%*	0.00	0.00	*0.0%*
(2) Total externalities	**0.0**	**0.0**	***0.0%***	**0.5**	**0.5**	***0.0%***	**0.5**	**0.5**	***0.0%***
(1) + (2) Total cost and externalities	**51.3**	**51.3**	***0.0%***	**62.8**	**62.8**	***0.0%***	**82.0**	**82.0**	***0.0%***
(3) Revenues from electricity generation	296.8	307.3	*-3.4%*	296.8	307.3	*-3.4%*	296.8	307.3	*-3.4%*
(1) - (3) Cost minus revenues	**-245.49**	**-255.92**	***-4.1%***	**-234.60**	**-245.03**	***-4.3%***	**-215.34**	**-225.76**	***-4.6%***
(1) + (2) - (3) Net societal cost of power generation	**-245.5**	**-255.9**	***-4.1%***	**-234.1**	**-244.5**	***-4.3%***	**-214.8**	**-225.3**	***-4.6%***

Table 9 continued: Integrated CBA for climate impacts on transmission lines

3 Bibliography

Acclimatise. (2009). *Building Business Resilience to Inevitable Climate Change. Carbon Disclosure Project Report. Global Electric Utilities.* Oxford.

Adeh, E. H., Good, S. P., Calaf, M., & Higgins, C. W. (2019). Solar PV Power Potential is Greatest Over Croplands. *Scientific reports, vol(9), no(1)*, pp. 1-6.

Ahsan, S., Rahman, M. A., Kaneco, S., Katsumata, H., Suzuki, T., & Ohta, K. (2005). Effect of temperature on wastewater treatment with natural and waste materials. *Clean Technologies and Environmental Policy, 7(3)*, 198-202.

Akbari, H. (2005). *Energy saving potentials and air quality benefits of urban heat island mitigation.* Récupéré sur OSTI.org: https://www.osti.gov/biblio/860475/

Akbari, H., Davis, S., Dorsano, S., Huang, J., & Winnett, S. (1992). *Cooling our communities: A guidebook on tree planting and light-colored surfacing.* Washington, DC (United States): Lawrence Berkeley Lab.; Environmental Protection Agency.

Alam, T., Mahmoud, A., Jones, K. D., Bezares-Cruz, J. C., & Guerrero, J. (2019). A Comparison of Three Types of Permeable Pavements for Urban Runoff Mitigation in the Semi-Arid South Texas, USA. *MDPI - Water, 11(10)*.

Allen, R. G., Pereira, L. S., Raes, D., & Smith, M. (2006). *FAO Irrigation and Drainage Paper - Crop Evapotranspiration.* FAO.

Allos, M. (2016, Juin). *Potential Damage Caused by Direct Lightning Strikes*. Récupéré sur Sollatek: https://www.sollatek.com/potential-damage-caused-direct-lightning-strikes/

American Society of Landscape Architects. (2003). *Chicago City Hall Green Roof*. Récupéré sur asla.org: http://www.asla.org/meetings/awards/awds02/chicagocityhall.html

Asian Development Bank. (2012). *Adaptation to Climate Change - The Case of a Combined Cycle Power Plant.* Philippines.

Attia, S. I. (2015). The influence of condenser cooling water temperature on the thermal efficiency of a nuclear power plant. *Annals of Nuclear Energy*, 371-378.

Bartos, M., Chester, M., Johnson, N., Gorman, B., Eisenberg, D., Linkov, I., & Bates, M. (2016). Impacts of rising air temperatures on electric transmission ampacity and peak electricity load in the United States. *Environmental Research Letters, 11(11), 1*.

Basha, M., Shaahid, S. M., & Al-Hadhrami, L. (2011). Impact of fuels on performance and efficiency of gas turbine power plants. *2nd International Conference on Advances in Energy Engineering*, (pp. 558-565). Bangkok.

Bassi, A. M., Pallaske, G., Wuennenberg, L., Graces, L., & Silber, L. (2019, March). *Sustainable Asset Valuation Tool: Natural Infrastructure.* Récupéré sur International Institute for Sustainable Development : https://www.iisd.org/sites/default/files/publications/sustainable-asset-valuation-tool-natural-infrastructure.pdf

Bengtson, H. (2020). *The Rational Method for Estimation of Design Surface Runoff Rate for Storm Water Control*. Récupéré sur brighthubengineering.com: https://www.brighthubengineering.com/hydraulics-civil-engineering/60842-the-rational-method-for-calculation-of-peak-storm-water-runoff-rate/

Bergel-Hayat, R., Debbarh, M., Antoniou, C., & Yannis, G. (2013). Explaining the road accident risk: weather effects. *Accident Analysis & Prevention, 60*, 456-465.

Berghage, R. D., Beattie, D., Jarrett, A. R., Thuring, C., Razaei, F., & O'Connor, T. P. (2009). *Green Roofs For Stormwater Runoff Control.* Cincinnati: EPA.

Bhatt, S., & Rajkumar, N. (2015). Effect of moisture in coal on station heat rate and fuel cost for Indian thermal power plants. *Power Research, 11(4)*, 773-786.

Bhattacharya, C., & Sengupta, B. (2016). Effect of ambient air temperature on the performance of regenerative air preheater of pulverised coal fired boilers. *Int. J. Energy Technology and Policy, Vol. 12, No. 2*, pp. 136–153.

Biswas, B. (2014). Construction and Evaluation of Rainwater Harvesting System for Domestic Use in a Remote and Rural Area of Khulna, Bangladesh. *International Scholarly Research Notices*. doi:https://doi.org/10.1155/2014/751952

Brouwer, C., & Heibloem, M. (1986). Irrigation Water Management and Irrigation Water Needs. *FAO - Training manual, 3.*

Brouwer, C., Prins, K., & Heibloem, M. (1989). *Irrigation water management: irrigation scheduling.* Récupéré sur Fao.org: http://www.fao.org/3/T7202E/t7202e00.htm#Contents

Büyükalaca, O., Bulut, H., & Yılmaz, T. (2001). Analysis of variable-base heating and cooling degree-days for Turkey. *Applied Energy, 69(4)*, pp. 269-283.

Carnegie Mellon University (CMU). (s.d.). *Integrated Environmental Control Model.* Récupéré sur Department of Engineering & Public Policy (EPP): https://www.cmu.edu/epp/iecm/

Chinowsky, P. S., Price, J. C., & Neumann, J. E. (2013). Assessment of climate change adaptation costs for the US road network. *Global Environmental Change, 23(4)*, 764-773.

Chinowsky, P., Hayles, C., Schweikert, A., Strzepek, N., Strzepek, K., & Schlosser, A. (2011). Climate change: comparative impact on developing and developed countries. *The Engineering Project Organization Journal*, pp. 67-80.

Choi, T., Keith, L., Hocking, E., Friedman, K., & Matheu, E. (2011). *Dams and energy sectors interdependency study.*

City of Chicago Department of Environment. (2006). *Green roof test plot project: annual project summary report.* Chicago.

Colman, J. (2013, Avril 26). The effect of ambient air and water temperature on power plant efficiency. *Master Thesis*. Duke University Libraries.

Cronshey, R., McCuen, R. H., Miller, N., Rawls, W., Robbins, S., & Woodward, D. (1986, June). *Urban Hydrology for Small Watersheds.* Récupéré sur USDA-United States Department of Agriculture: https://www.nrcs.usda.gov/Internet/FSE_DOCUMENTS/stelprdb1044171.pdf

Das, T. K., Saharawat, Y. S., Bhattacharyya, R., Sudhishri, S., Bandyopadhyay, K. K., Sharma, A. R., & Jat, M. L. (2018). Conservation agriculture effects on crop and water productivity, profitability and soil organic carbon accumulation under a maize-wheat cropping system in the North-western Indo-Gangetic Plains. *Field Crops Research, 215*, pp. 222-231.

Davies, Z. G., Edmondson, J. L., Heinemeyer, A., Leake, J. R., & Gaston, K. J. (2011). Mapping an urban ecosystem service: quantifying above-ground carbon storage at a city-wide scale. *Journal of applied ecology, 48(5)*, pp. 1125-1134.

Davy, R., Gnatiuk, N., Pettersson, L., & Bobylev, L. (2018). Climate change impacts on wind energy potential in the European domain with a focus on the Black Sea. *Renewable and sustainable energy reviews*, pp. 1652-1659.

De Oliveira, V., De Mello, C., Viola, M., & Srinivasan, R. (2017). Assessment of climate change impacts on the streamflow and hydropower potential in the headwater region of the Grande river basin, Southeastern Brazil. *International Journal of Climatology 37[15]*, pp. 5005-5023.

De Rosa, M., Bianco, V., Scarpa, F., & Tagliafico, L. A. (2014). Heating and cooling building energy demand evaluation; a simplified model and a modified degree days approach. *Applied Energy, 128*, 217-229.

De Sa, A., & Al Zubaidy, S. (2011). Gas turbine performance at varying ambient temperature. *Applied Thermal Engineering, 31(14-15)*, 2735-2739.

Demuzere, M., Orru, K., Heidrich, O., Olazabal, E., Geneletti, D., Orru, H., . . . Faehnle, M. (2014). Mitigating and adapting to climate change: Multi-functional and multi-scale assessment of green urban infrastructure. *Journal of environmental management, 146*, pp. 107-115.

Dhakal, S., & Hanaki, K. (2002). Improvement of urban thermal environment by managing heat discharge sources and surface modification in Tokyo. *Energy and buildings, 34(1)*, pp. 13-23.

Diaz, C. A., Osmond, P., & King, S. (2015). Precipitation and buildings: estimation of the natural potential of locations to sustain indirect evaporative cooling strategies through hot seasons. *Living and Learning: Research for a Better Built Environment: 49th International Conference of the Architectural Science Association*, (pp. 45-54). Melbourne.

Djaman, K., O'Neill, M., Owen, C. K., Smeal, D., Koudahe, K., West, M., & Irmak, S. (2018). Crop evapotranspiration, irrigation water requirement and water productivity of maize from meteorological data under semiarid climate. *MDPI - Water 2018, 10(4), 405*.

Doorenbos, J., & Kassam, A. (1979). *Yield response to Water Irrigation and Drainage.* Roma: Food and Agricultural Organization; Paper No 33.

Drax. (2017, August 29). *Technology - What hot weather means for electricity*. Récupéré sur Drax.com: https://www.drax.com/technology/hot-weather-means-electricity/

Du, L., Trinh, X., Chen, Q., Wang, C., Wang, H., Xia, X., . . . Wu, Z. (2018). Enhancement of microbial nitrogen removal pathway by vegetation in Integrated Vertical-Flow Constructed Wetlands (IVCWs) for treating reclaimed water. *Bioresource technology, 2*.

Dunn, A. D. (2007). *Green light for green infrastructure.* Récupéré sur Digitalcommons.pace.edu: https://digitalcommons.pace.edu/lawfaculty/494

Durmayaz, A., & Sogut, O. S. (2006). Influence of cooling water temperature on the efficiency of a pressurized-water reactor nuclear-power plant. *International Journal of Energy Research, 30(10)*, pp. 799-810.

East Coast Lightning Equipment INC. (s.d.). *Lightning protection installation cost study* . Récupéré sur East Coast Lightning Equipment INC: https://ecle.biz/coststudy/

Eliasson, J., & Ludvigsson, G. (2000). Load factor of hydropower plants and its importance in planning and design. *11th International Seminar on Hydro Power Plants.* Vienna.

El-Refaie, G. (2010). Temperature impact on operation and performance of Lake. *Ain Shams Engineering Journal 1*, 1-9.

El-Shobokshy, M. S., & Hussein, F. M. (1993). Degradation of photovoltaic cell performance due to dust deposition on to its surface. *Renewable Energy, 3(6-7)*, pp. 585-590.

Engineering ToolBox. (2009). *Pumping Water - Energy Cost Calculator*. Récupéré sur engineeringtoolbox.com: https://www.engineeringtoolbox.com/water-pumping-costs-d_1527.html

Engineering ToolBox. (s.d.). *Hydropower*. Récupéré sur Engineering ToolBox: https://www.engineeringtoolbox.com/hydropower-d_1359.html

EPA. (2014). *The Economic Benefits of Green Infrastructure - A Case Study of Lancaster, PA.*

Eurostat. (2019). *Energy statistics - cooling and heating degree days (nrg_chdd)*. Récupéré sur Eurostat, the Statistical Office of the European Union: https://ec.europa.eu/eurostat/cache/metadata/en/nrg_chdd_esms.htm

Eurostat, the Statistical Office of the European Union. (2019). *Energy statistics - cooling and heating degree days (nrg_chdd)*. Récupéré sur Europa.eu: https://ec.europa.eu/eurostat/cache/metadata/en/nrg_chdd_esms.htm

Evans, D. V., & Antonio, F. D. (1986). Hydrodynamics of Ocean Wave-Energy Utilization: IUTAM Symposium Lisbon/Portugal 1985. *Springer Science & Business Media*, pp. 133-156.

Farkas, Z. (2011). *Considering air density in wind power production.* Budapest.

Fisher, J. C., Bartolino, J. R., Wylie, A. H., Sukow, J., & McVay, M. (2016). *Groundwater-flow model for the Wood River Valley aquifer system, south-central Idaho.* US Geological Survey.

Flowers, M. E., Smith, M. K., Parsekian, A. W., Boyuk, D. S., McGrath, J. K., & Yates, L. (2016). Climate impacts on the cost of solar energy. *Energy Policy, 94*, pp. 264-273.

Gajbhiye, S., Mishra, S. K., & Pandey, A. (2013). Effects of Seasonal/Monthly Variation on Runoff Curve Number for Selected Watersheds of Narmada Basin. *International Journal of Environmental Sciences, Volume 3, No 6*, pp. 2019-2030.

Garfí, M., Pedescoll, A., Bécares, E., Hijosa-Valsero, M., Sidrach-Cardona, R., & García, J. (2012). Effect of climatic conditions, season and wastewater quality on contaminant removal efficiency of two experimental constructed wetlands in different regions of Spain. *Science of the total environment, 437*, pp. 61-67.

Georgi, N. J., & Zafiriadis, K. (2006). The impact of park trees on microclimate in urban areas. *Urban Ecosystems, 9(3)*, pp. 195-209.

Ghamami, M., Fayazi Barjin, A., & Behbahani, S. (2016). Performance Optimization of a Gas Turbine Power Plant Based on Energy and Exergy Analysis. *Mechanics, Materials Science & Engineering Journal, 29*.

GIZ. (2016). *Solar Powered Irrigation Systems (SPIS) – Technology, Economy, Impacts.* Récupéré sur Gesellschaft für Internationale Zusammenarbeit (GIZ): https://energypedia.info/images/temp/2/23/20160630122544!phpeKHVUr.pdf

Gomes, J., Diwan, L., Bernardo, R., & Karlsson, B. (2014). Minimizing the Impact of Shading at Oblique Solar Angles in a Fully Enclosed Asymmetric Concentrating PVT Collector. *Energy Procedia (57)*, pp. 2176-2185.

Good, E., & Calaf, S. (2019). Solar PV Power Potential is Greatest Over Croplands. *SciRep (9, 11442)*.

Green, A. (2020). *The intersection of energy and machine learning*. Récupéré sur adgefficiency.com: https://adgefficiency.com/energy-basics-ambient-temperature-impact-on-gas-turbine-performance/

Haerter, J., Hagemann, S., Moseley, C., & Piani, C. (2011). Climate model bias correction and the role of timescales. *Hydrology and Earth System Sciences, 15*, pp. 1065-1073.

Handayani, K., Filatova, T., & Krozer, Y. (2019). The Vulnerability of the Power Sector to Climate Variability and Change: Evidence from Indonesia. *Energies, 12(19), 3640*.

Harrison, G. P., & Whittington, H. W. (2002). Vulnerability of hydropower projects to climate change. *IEE proceedings-generation, transmission and distribution, 149(3)*, pp. 249-255.

Harrison, G., & Wallace, A. (2005). Climate sensitivity of marine energy. *Renewable Energy, 30(12)*, pp. 1801-1817.

Henry, C. L., & Pratson, L. F. (2016). Effects of environmental temperature change on the efficiency of coal-and natural gas-fired power plants. *Environmental science & technology, 50(17)*, 9764-9772.

Hutyra, L. R., Yoon, B., & Alberti, M. (2011). Terrestrial carbon stocks across a gradient of urbanization: a study of the Seattle, WA region. *Global Change Biology, 17(2)*, pp. 783-797.

Ibrahim, S., Ibrahim, M., & Attia, S. (2014). The impact of climate changes on the thermal performance of a proposed pressurized water reactor: nuclear-power plant. *International Journal of Nuclear Energy*.

Jabboury, B. G., & Darwish, M. A. (1990). Performance of gas turbine co-generation power desalting plants under varying operating conditions in Kuwait. *Heat Recovery Systems and CHP, 10(3)*, 243-253.

Jackson, N., & Puccinelli, J. (2006). *Long-Term Pavement Performance (LTPP) data analysis support: National pooled fund study TPF-5 (013)-effects of multiple freeze cycles and deep frost penetration on pavement performance and cost (No. FHWA-HRT-06-121).*

Janssen, H., Carmeliet, J., & Hens, H. (2004). The influence of soil moisture transfer on building heat loss via the ground. *Building and Environment, 39(7)*, 825-836.

Jerez, S., Tobin, I., Vautard, R., Montávez, J. P., López-Romero, J. M., Thais, F., . . . Wild, M. (2015). The impact of climate change on photovoltaic power generation in Europe. *Nature Communications, 6(1)*, pp. 1-8.

Ji, M., Hu, Z., Hou, C., Liu, H., Ngo, H. H., Guo, W., . . . Zhang, J. (2020). New insights for enhancing the performance of constructed wetlands at low temperatures. *Bioresource Technology, 122722*.

JICA. (March 2003). *Manual on flood control planning.* Department of public works and highways.

Jim, C. Y., & Chen, W. Y. (2008). Assessing the ecosystem service of air pollutant removal by urban trees in Guangzhou (China). *Journal of environmental management, 88(4)*, pp. 665-676.

Kadlec, R. H., & Reddy, K. R. (2001). Temperature effects in treatment wetlands. *Water environment research, 73(5)*, pp. 543-557.

Kakaras, E., Doukelis, A., Prelipceanu, A., & Karellas, S. (2006). Inlet air cooling methods for gas turbine based power plants.

Kaldellis, J., & Fragos, P. (2011). Ash deposition impact on the energy performance of photovoltaic generators. *Journal of cleaner production, 19(4)*, pp. 311-317.

Kappos, L., Ntouros, I., & Palivos, I. (1996). Pollution effect on PV system efficiency. *Proceedings of the 5th National Conference on Soft Energy Forms.* Athens.

Kivi, R. (2017, Avril 24). *How Does Geothermal Energy Work?* Récupéré sur Sciencing: https://sciencing.com/geothermal-energy-work-4564716.html

Kloss, C., & Calarusse, C. (2011). *Rooftops to Rivers: Green strategies for controlling stormwater and combined sewer overflows.* New-York.

Koc, C. B., Osmond, P., & Peters, A. (2018). Evaluating the cooling effects of green infrastructure: A systematic review of methods, indicators and data sources. *Solar Energy, 166*, pp. 486-508.

Koch, H., & Vögele, S. (2009). Dynamic modelling of water demand, water availability and adaptation strategies for power plants to global change. *Ecological Economics, 68(7)*, pp. 2031-2039.

Kosa, P. (2011). The effect of temperature on actual evapotranspiration based on Landsat 5 TM Satellite Imagery. *Evapotranspiration, 56(56)*, pp. 209-228.

Krishna, P., Kumar, K., & Bhandari, N. M. (2002). IS: 875 (Part3): Wind loads on buildings and structures-proposed draft & commentary. Document No.: IITK-GSDMA-Wind, 02-V5. Roorkee, Uttarakhand, India: Department of Civil Engineering; Indian Institute of Technology Roorkee.

Kumpulainen, L., Laaksonen, H., Komulainen, R., Martikainen, A., Lehtonen, M., Heine, P., . . . Saaristo, H. (2007). *Distribution Network 2030 - Vision of the future power system.* Finland: VTT.

Land, M., Granéli, W., Grimvall, A., Hoffmann, C. C., Mitsch, W. J., Tonderski, K. S., & Verhoeven, J. T. (2016). How effective are created or restored freshwater wetlands for nitrogen and phosphorus removal? A systematic review. *Environmental Evidence, 5*.

Larsen, P., Goldsmith, S., Wilson, M., Strzepek, K., Chinowsky, P., & Saylor, B. (2008). Estimating future costs for Alaska public infrastructure at risk from climate. *Global Environmental Change*, pp. 442-457.

Lavin, P. (2003). *A Practical Guide to Design, Production, and Maintenance for Architects and Engineers.* London/New-York: Spon Press.

Law, Y., Ye, L., Pan, Y., & Yuan, Z. (2012). Nitrous oxide emissions from wastewater treatment processes. *Philosophical Transactions of the Royal Society B: Biological Sciences, 367(1593)*, pp. 1265-1277.

Linnerud, K., Mideksa, T. K., & Eskeland, G. S. (2011). The impact of climate change on nuclear power supply. *The Energy Journal, 32(1)*.

Lise, W., & van der Laan, J. (2015). Investment needs for climate change adaptation measures of electricity power plants in the EU. *Energy for Sustainable Development, 28*, pp. 10-20.

Mamo, G. E., Marence, M., Hurtado, J. C., & Franca, M. J. (2018). Optimization of Run-of-River Hydropower Plant Capacity.

Manoli, G., Fatichi, S., Schläpfer, M., Yu, K., Crowther, T. W., Meili, N., . . . Bou-Zeid, E. (2019). Magnitude of urban heat islands largely explained by climate and population. *Manoli, G., Fatichi, S., Schläpfer, M., Yu, K., Crowther, T. W., Meili, N., ... & Bou-Zeid, E. (2019). Magnitude of urban Nature, 573(7772)*, pp. 55-60.

Manwell, J. F., McGowan, J. G., & Rogers, A. L. (2010). *Wind energy explained: theory, design and application.* John Wiley & Sons.

Manwell, J., McGowan, J., & Rogers, A. (2002). *Wind Energy Explained: Theory, Design and Application.*

Maulbetsch, J. S., & Di Filippo, M. N. (2006). *Cost and value of water use at combined-cycle power plants.* California: California Energy Commission - Public Interest Energy Research Program.

Maupoux, M. (2010). *Solar photovoltaic water pumping.* Récupéré sur Practical Action - The Schumacher Centre for Technology and Development :

https://sswm.info/sites/default/files/reference_attachments/MAUPOUX%202010%20Solar%20Water%20Pumping.pdf

Meral, M. E., & Dincer, F. (2011). A review of the factors affecting operation and efficiency of photovoltaic based electricity generation systems. *Renewable and Sustainable Energy Reviews, 15(5)*, pp. 2176-2184.

Mimikou, M. A., & Baltas, E. A. (1997). Climate change impacts on the reliability of hydroelectric energy production. *Hydrological Sciences Journal, 42(5)*, pp. 661-678.

Miradi, M. (2004). Artificial neural network (ANN) models for prediction and analysis of ravelling severity and material composition properties. *CIMCA*, pp. 892-903.

Mirgol, B., Nazari, M., & Eteghadipour, M. (2020). Modelling Climate Change Impact on Irrigation Water Requirement and Yield of Winter Wheat (Triticum aestivum L.), Barley (Hordeum vulgare L.), and Fodder Maize (Zea mays L.) in the Semi-Arid Qazvin Plateau, Iran. *Agriculture, 10(3), 60*.

Mourshed, M. (2012). Relationship between annual mean temperature and degree-days. *Energy and buildings, 54*, pp. 418-425.

N.D. Lea International. (1995). *Modelling Road Deterioration and Maintenance.* Prepared for the Asian Development Bank.

N.D. Lea International. (1995). *Modelling Road Deterioration and Maintenance.* Prepared for the Asian Development Bank.

National Snow & Ice Data Center. (n.d.). *freezing degree-days*. Retrieved from https://nsidc.org/cryosphere/glossary/term/freezing-degree-days

Nazahiyah, R., Yusop, Z., & Abustan, I. (2007). Stormwater quality and pollution loading from an urban residential catchment in Johor, Malaysia. *Water science and technology, 56(7)*, pp. 1-9.

Nemry, F., & Demirel, H. (2012). *Impacts of Climate Change on Transport: A focus on road and rail transport infrastructures.* Luxembourg: Publications Office of the European Union.

Nichol, J. E. (1996). High-resolution surface temperature patterns related to urban morphology in a tropical city: A satellite-based study. *Journal of applied meteorology, 35(1)*, pp. 135-146.

Nordhaus, W. (2017). Revisiting the social cost of carbon. *PNAS*, vol. 11, no.7, 1518-1523.

Nowak, D. J., Greenfield, E. J., Hoehn, R. E., & Lapoint, E. (2013). Carbon storage and sequestration by trees in urban and community areas of the United States. *Environmental pollution, 178, 229-236.*, pp. 229-236.

Ould-Amrouche, S., Rekioua, D., & Hamidat, A. (2010). Modelling photovoltaic water pumping systems and evaluation of their CO2 emissions mitigation potential. *Applied Energy, 87*, pp. 3451-3459.

Panagea, I. S., Tsanis, I. K., Koutroulis, A. G., & Grillakis, M. G. (2014). Climate change impact on photovoltaic energy output: the case of Greece. *Advances in Meteorology*.

Pande, P., & Telang, S. (2014). Calculation of Rainwater Harvesting Potential by Using Mean Annual Rainfall, Surface Runoff and Catchment Area. *Green Clean Guide, India, Global Advanced Research Journal of Agricultural Science, Vol 3(7)*, 200-204.

Parker, J. H. (1989, February). The impact of vegetation on air conditioning consumption. *In Proceedings of the Workshop on Saving Energy and Reducing Atmospheric Pollution by Controlling Summer Heat Islands (pp. 45-52).*

Parliamentary Office of Science and Technology (POST). (2011). *Carbon footprint of electricity generation.* Récupéré sur POST Note Update, 383: https://www.parliament.uk/documents/post/postpn_383-carbon-footprint-electricity-generation.pdf

Pérez, G., Coma, J., Martorell, I., & Cabeza, L. F. (2014). Vertical Greenery Systems (VGS) for energy saving in buildings: A review. *Renewable and Sustainable Energy Reviews, 39*, pp. 139-165.

Petchers, N. (2003). *Combined heating, cooling & power handbook: technologies & applications: an integrated approach to energy resource optimization.* Fairmont Press.

Photovoltaic Softwares. (2020). *Photovoltaic Softwares*. Récupéré sur photovoltaic-software.com: https://photovoltaic-software.com/principle-ressources/how-calculate-solar-energy-power-pv-systems

Pierson Jr, W., & Moskowitz, L. (1964). A proposed spectral form for fully developed wind seas based on the similarity theory of SA Kitaigorodskii. *Journal of geophysical research*, pp. 5181-5190.

Plósz, B. G., Liltved, H., & Ratnaweera, H. (2009). Climate change impacts on activated sludge wastewater treatment: a case study from Norway. *Water Science and Technology, 60(2)*, pp. 533-541.

Poullain, J. (2012). *PDHonline Course H119 (2 PDH) - Estimating Storm Water Runoff.* Récupéré sur pdhonline.org: https://pdhonline.com/courses/h119/stormwater%20runoff.pdf

Prado, R. T., & Ferreira, F. L. (2005). Measurement of albedo and analysis of its influence the surface temperature of building roof materials. *Energy and Buildings, 37(4)*, 295-300.

Rademaekers, K., van der Laan, J., Boeve, S., Lise, W., van Hienen, J., Metz, B., . . . Kirchsteiger, C. (2011). *Investment needs for future adaptation measures in EU nuclear power plants and other electricity generation technologies due to effects of climate change* . Brussels: Library (DM28, 0/36).

Ramos-Scharron, C., & MacDonald, L. (2007). Runoff and suspended sediment yields from an unpaved road segment. *Hydrological Processes, 21(1)*, pp. 35-50.

Rodell, M., Chen, J., Kato, H., Famiglietti, J. S., Nigro, J., & Wilson, C. R. (2007). Estimating groundwater storage changes in the Mississippi River basin (USA) using GRACE. *Hydrogeology Journal 15[1]*, pp. 159-166.

Roorda, J., & van der Graaf, J. (2000). Understanding membrane fouling in ultrafiltration of WWTP-effluent. *Water Science and Technology 41(10-11)*, pp. 345-353.

Rousseau, Y. (2013). Impact of Climate Change on Thermal Power Plants. Case study of thermal power plants in France.

Sahely, H. R., MacLean, H. L., Monteith, H. D., & Bagley, D. M. (2006). Comparison of on-site and upstream greenhouse gas emissions from Canadian municipal wastewater treatment facilities. *Journal of Environmental Engineering and Science, 5(5)*, pp. 405-415.

Saito, I., Ishihara, O., & Katayama, T. (1990). Study of the effect of green areas on the thermal environment in an urban area. *Energy and buildings, 15(3-4)*, pp. 493-498.

Santamouris, M. (2014). Cooling the cities–a review of reflective and green roof mitigation technologies to fight heat island and improve comfort in urban environments. *Solar energy, 103*, pp. 682-703.

Scheehle, E. A., & Doorn, M. R. (2012). *Estimate of United States GHG Emissions from wastewater.* Récupéré sur EPA.org: https://www3.epa.gov/ttn/chief/conference/ei12/green/present/scheele.pdf

Scheehle, E. A., & Doorn, M. R. (2012). *Improvements to the U.S. Wastewater Methane and Nitrous Oxide Emissions.* Récupéré sur EPA.org: https://www3.epa.gov/ttn/chief/conference/ei12/green/scheehle.pdf

Schnetzer, J., & Pluschke, L. (2017). *Solar-Powered Irrigation Systems: A clean-energy, low-emission option for irrigation development and modernization.* FAO.

Shukla, A. K., & Singh, O. (2014). Effect of Compressor Inlet Temperature & Relative Humidity on Gas Turbine Cycle Performance. *International Journal of Scientific & Engineering Research, 5(5)*, 664-670.

Shukla, A. K., & Singh, O. (2014). Effect of Compressor Inlet Temperature & Relative Humidity on Gas Turbine Cycle Performance. *International Journal of Scientific & Engineering Research, 5(5)*, 664-670.

Singh, S., & Kumar, R. (2012). Ambient air temperature effect on power plant performance. *International Journal of Engineering Science and Technology*.

Singh, S., & Tiwari, S. (2019). *Climate Change, Water and Wastewater Treatment: Interrelationship and Consequences.* Singapore: Springer.

Song, Z., Zheng, Z., Li, J., Sun, X., Han, X., Wang, W., & Xu, M. (2006). Seasonal and annual performance of a full-scale constructed wetland system for sewage treatment in China. *Ecological Engineering, 26(3)*, pp. 272-282.

Souch, C. A., & Souch, C. (1993). The effect of trees on summertime below canopy urban climates: a case study Bloomington. *Journal of Arboriculture, 19(5)*, pp. 303-312.

Taha, H. (1996). Modeling impacts of increased urban vegetation on ozone air quality in the South Coast Air Basin. *Atmospheric Environment, 30(20)*, pp. 3423-3430.

Taha, H. (1997). Urban climates and heat islands; albedo, evapotranspiration, and anthropogenic heat. *Energy and buildings, 25(2).*

Taha, H., Akbari, H., & Rosenfeld, A. (1988). Vegetation Canopy Micro-Climate: A Field-Project in Davis, California. *Journal of Climate and Applied Meteorology*.

Taha, H., Akbari, H., & Rosenfeld, A. (1991). Heat island and oasis effects of vegetative canopies: micro-meteorological field-measurements. *Theoretical and Applied Climatology, 44(2)*, pp. 123-138.

Tallis, M., Taylor, G., Sinnett, D., & Freer-Smith, P. (2011). Estimating the removal of atmospheric particulate pollution by the urban tree canopy of London, under current and future environments. *Landscape and Urban Planning, 103(2)*, pp. 129-138.

Tang, H. (2012). Research on Temperature and Salt Migration Law of Sulphate Salty Soil Subgrade in Xinjiang Region. Beijing, China: Beijing Jiaotong University.

Taylor, C. R., Hook, P. B., Stein, O. R., & Zabinski, C. A. (2011). Seasonal effects of 19 plant species on COD removal in subsurface treatment wetland microcosms. *Ecological Engineering, 37(5)*, pp. 703-710.

Tiwary, A., Sinnett, D., Peachey, C., Chalabi, Z., Vardoulakis, S., Fletcher, T., . . . Hutchings, T. R. (2009). An integrated tool to assess the role of new planting in PM10 capture and the human health benefits: A case study in London. *Environmental pollution, 157(10)*, pp. 2645-2653.

Tran, Q. K., Jassby, D., & Schwabe, K. A. (2017). The implications of drought and water conservation on the reuse of municipal wastewater: Recognizing impacts and identifying mitigation possibilities. *Water research, 124*, 472-481.

Tsihrintzis, V. A., & Hamid, R. (1998). Runoff quality prediction from small urban catchments using SWMM. *Hydrological Processes, 12(2)*, pp. 311-329.

U.S. DoE. (2013). *U.S. Energy sector vulnerabilities to climate change and extreme weather.* DOE/PI-0013: U.S. Department of Energy.

U.S. Environmental Protection Agency. (2003, September). *Cooling summertime temperatures: Strategies to reduce heat islands.* Récupéré sur epa.gov: https://www.epa.gov/sites/production/files/2014-06/documents/hiribrochure.pdf

Ullrich, A., & Volk, M. (2009). Application of the Soil and Water Assessment Tool (SWAT) to predict the impact of alternative management practices on water quality and quantity. *Agricultural Water Management, 96(8)*, pp. 1207-1217.

UNEP. (2015). *Economic Valuation of Wastewater - The Cost of Action and the Cost of No Action.* United Nations Environment Programme (UNEP), commissioned by the Global Programme of Action for the Protection of the Marine Environment from Land-based Activities (GPA), through the Global Wastewater Initiative (GW2I).

URS Corporation Limited. (2010). *Adapting Energy, Transport and Water Infrastructure to the Long-term Impacts of Climate Change .* San Francisco, CA, USA, Report RMP/5456.

Valkama, P., Mäkinen, E., Ojala, A., Vahtera, H., Lahti, K., Rantakokko, K., . . . Wahlroos, O. (2017). Seasonal variation in nutrient removal efficiency of a boreal wetland detected by high-frequency on-line monitoring. *Ecological engineering, 98*, pp. 307-317.

Van Vliet, M. T., Yearsley, J. R., Ludwig, F., Vögele, S., Lettenmaier, D. P., & Kabat, P. (2012). Vulnerability of US and European electricity supply to climate change. *Nature Climate Change, 2(9)*, 676-681.

Vought, T. D. (2019, June 30). *An Economic Case for Facility Lightning Protection Systems in 2017*. Récupéré sur VFC: https://vfclp.com/articles/an-economic-case-for-facility-lightning-protection-systems-in-2017/

Watkins, R., Littlefair, P., Kolokotroni, M., & Palmer, J. (2002). The London heat island–Surface and air temperature measurements in a park and street gorges. *ASHRAE Transactions, 108(1)*, pp. 419-427.

Wilbanks, T., Bhatt, V., Bilello, D., Bull, S., Ekmann, J., Horak, W., & Huang, Y. J. (2008). *Effects of Climate Change on Energy Production and Use in the United States.* Lincoln: US Department of Energy Publications.

Xiao, Q., & McPherson, E. G. (2002). Rainfall interception by Santa Monica's municipal urban forest. *Urban ecosystems, 6(4)*, pp. 291-302.

Yamba, F., Walimwipi, H., Jain, S., Zhou, P., Cuamba, B., & Mzezewa, C. (2011). Climate change/variability implications on hydroelectricity generation in the Zambezi River Basin. *Mitigation and Adaptation Strategies for Global Change*, pp. 617-628.

Young, I. R., & Holland, G. J. (1996). Atlas of the oceans: wind and wave climate. *Oceanographic Literature Review, 7(43), 742*.

Yuan, H., Nie, J., Zhu, N., Miao, C., & Lu, N. (2013). Effect of temperature on the wastewater treatment of a novel anti-clogging soil infiltration system. *Ecological engineering, 57*, pp. 375-379.

Zhang, C., Liao, H., & Mi, Z. (2019). Climate impacts: temperature and electricity consumption. *Natural Hazards, 99(3)*, pp. 1259-1275.

Zhang, Y., Kendy, E., Qiang, Y., Changming, L., Yanjun, S., & Hongyong, S. (2004). Effect of soil water deficit on evapotranspiration, crop yield, and water use efficiency in the North China Plain. *Agricultural Water Management, 64*(2), pp. 107-122.

Zhao, C., Liu, B., Piao, S., Wang, X., Lobell, D., Huang, Y., ... (2017). Temperature increase reduces global yields of major crops in four independent estimates. *Proceedings of the National Academy of Sciences, 114 (35)*. doi:https://doi.org/10.1073/pnas.1701762114

Zhao, M., Kong, Z. H., Escobedo, F. J., & Gao, J. (2010). Impacts of urban forests on offsetting carbon emissions from industrial energy use in Hangzhou, China. *Journal of Environmental Management, 91(4)*, pp. 807-813.

Zhao, X., Shen, A., & Ma, B. (2018). Temperature Adaptability of Asphalt Pavement to High Temperatures and Significant Temperature Differences. *Advances in Materials Science and Engineering*.

Zheng, S., Huang, G., Zhou, X., & Zhu, X. (2020). Climate-change impacts on electricity demands at a metropolitan scale: A case study of Guangzhou, China. *Applied Energy, 261, 114295*.

Zhou, Z. C., Shangguan, Z. P., & Zhao, D. (2006). Modeling vegetation coverage and soil erosion in the Loess Plateau Area of China. *Ecological modelling, 198(1-2)*, pp. 263-268.

Zoppou, C. (2001). Review of urban storm water models. *Environmental Modelling & Software, 16(3)*, pp. 195-231.

Zouboulis, A., & Tolkou, A. (2016). Effect of climate change in wastewater treatment plants: reviewing the problems and solutions. Dans S. A. Shrestha, *Managing Water Resources under Climate Uncertainty* (pp. 197-220). Springer.

Zoulia, I., Santamouris, M., & Dimoudi, A. (2009). Monitoring the effect of urban green areas on the heat island in Athens. *Environmental monitoring and assessment, 156(1-4)*.

Zsirai, T., Buzatu, P., Maffettone, R., & Judd, S. (2012, April). *Sludge viscosity—The thick of it*. Récupéré sur The MBR (Membrane Bioreactors): https://www.thembrsite.com/features/sludge-viscosity-in-membrane-bioreactors-the-thick-of-it/

Annex I: Code for establishing the CDS Toolbox-SAVi link

Code related to offline processing of CDS Toolbox and CDS API data for the C3S_428h_IISD-EU project.

How does this code relate to the CDS API ?

This code builds on the powerful CDS API but focuses on local impact analysis specific for the C3S_428h_IISD-EU project. It makes it easier to retrieve a time series for a specific location or region, and save the result to a CSV file (a simpler format than netCDF for most climate adaptation practitioners). Additionally, the code combines variables across multiple datasets, aggregate them into asset classes (such as all energy-related variables) and perform actions such as bias correction (use of ERA5 and CMIP5).

Code available for download

The easy way is to download the zipped archive: - latest (development): https://github.com/perrette/iisd-cdstoolbox/archive/master.zip - or check stable releases with description of changes: https://github.com/perrette/iisd-cdstoolbox/releases (see assets at the bottom of each release to download a zip version)

The hacky way is to use git (only useful during development, for frequent updates, to avoid having to download and extract the archive every time):

- First time: `git clone https://github.com/perrette/iisd-cdstoolbox.git`

- Subsequent updates: `git pull` from inside the repository

Installation steps

- Download the code (see above) and inside the folder.
- Install Python 3, ideally Anaconda Python which comes with pre-installed packages
- Install the CDS API key: https://cds.climate.copernicus.eu/api-how-to
- Install the CDS API client: pip install cdsapi
- Install other dependencies: conda install --file requirements.txt or pip install -r requirements.txt
- *Optional* dependency for coastlines on plots: conda install -c conda-forge cartopy or see docs
- *Optional* dependency: CDO (might be needed later, experimental): conda install -c conda-forge python-cdo

Troubleshooting: - If install fails, you may need to go through the dependencies in requirements.txt one by one and try either pip install or conda install or other methods specific to that dependency. - In the examples that follow, if you have both python2 and python3 installed, you might need to replace python with python3.

CDS API

Download indicators associated with one asset class.

Examples of use:

```
python download.py --asset energy --location Welkenraedt
```

The corresponding csv time series will be stored in `indicators/welkenraedt/energy`. Note that raw downloaded data from the CDS API (regional tiles in netcdf format, and csv for the required lon/lat, without any correction) are stored under `download/` and can be re-used across multiple indicators.

The `indicators` folder is organized by location, asset class, simulation set and indicator name. The aim is to provide multiple sets for SAVi simulation. For instance, `era5` for past simulations, and various `cmip5` versions for future simulations, that may vary with model and experiment. For instance the above command creates the folder structure (here a subset of all variables is shown):

```
indicators/
  welkenraedt/
    energy/
      era5/
        2m_temperature.csv
        precipitation.csv
        ...
      cmip5-ipsl_cm5a_mr-rcp_8_5/
        2m_temperature.csv
        precipitation.csv
        ...
      ...
```

with two simulation sets `era5` and `cmip5-ipsl_cm5a_mr-rcp_8_5`. It is possible to specify other models and experiment via `--model` and `--experiment` parameters, to add further simulation sets and thus test how the choice of climate models and experiment affect the result of SAVi simulations.

Compared to raw CDS API, some variables are renamed and scaled so that units match and are the same across simulation sets. For instance, temperature was adjusted from Kelvin to degree Celsius, and precipitation was renamed and units-adjusted into mm per month from original (mean_total_precipitation_rate (mm/s) in ERA5, and mean_precipitation_flux (mm/s) in CMIP5). Additionally, CMIP5 data is corrected so that climatological mean matches with ERA5 data (climatology computed over 1979-2019 by default).

Additionally to the files shown in the example folder listing above, figures can also be created for rapid control of the data, either for interactive viewing (`--view-timeseries` and `--view-region`) or or saved as PNG files (`--png-timeseries` and `--png-region`), e.g.

```
python download.py --asset energy --location Welkenraedt --png-timeseries --
png-region
```

Single indicators can be downloaded via:

```
python download.py --indicator 2m_temperature --location Welkenraedt
```

The choices available for `--indicator` , `--asset` and `--location` area defined in the following configuration files, respectively:

- controls which indicators are available, how they are renamed and unit-adjusted: indicators.yml (see sub-section below)
- controls the indicator list in each asset class: assets.yml
- controls the list of locations available: locations.yml

Full documentation, including fine-grained controls, is provided in the command-line help:

```
python download.py --help
```

Visit the CDS Datasets download pages, for more information about available variables, models and scenarios:

- ERA5: https://cds.climate.copernicus.eu/cdsapp#!/dataset/reanalysis-era5-single-levels-monthly-means?tab=form

- CMIP5: https://cds.climate.copernicus.eu/cdsapp#!/dataset/projections-cmip5-monthly-single-levels?tab=form

In particular, clicking on “Show API request” provides information about spelling of the parameters, e.g. that “2m temperature” is spelled `2m_temperature` and “RCP 8.5” is spelled `rcp_8_5`.

Indicator definition

This section is intended for users who wish to extend the list of indicators currently defined in indicators.yml. It can be safely ignored for users who are only interested in using the existing indicators.

Let’s see how `10m_wind_speed` is defined:

```
- name: 10m_wind_speed
  units: m / s
  description: Wind speed magnitude at 10 m
```

The fields `name` and `units` define the indicator. Description is optional, just to provide some context. It is possible to provide `scale` and `offset` fields to correct the data as `(data + offset) * scale`. Here for `2m temperature`:

```
- name: 2m_temperature
  units: degrees Celsius
  description: 2-m air temperature
  offset: -273.15  # Kelvin to degrees C
```

# denotes a comment to provide some context. Some indicators have different names in ERA5 and CMIP5, and possibly different units. That can be dealt with by providing `era5` and `cmip5` fields, which have precedence over the top-level fields. Here the `evaporation` definition:

```
- name: evaporation
  units: mm per month
  era5:
    name: mean_evaporation_rate  # different name in ERA5
    scale: -2592000  # change sign and convert from mm/s to mm / month
  cmip5:
    scale: 2592000  # mm/s to mm / month
```

In that case both scaling and name depend on the dataset. In CMIP5 which variable name is identical to our indicator name, the `name` field can be omitted. In ERA5, evaporation is negative (downwards fluxes are counted positively), whereas it is counted positively in ERA5.

Indicators composed of several CDS variables can be defined via `compose` and `expression` fields. Let's look at `100m_wind_speed`:

```
- name: 100m_wind_speed
  units: m / s
  description: Wind speed magnitude at 100 m
  era5:
    compose:
      - 100m_u_component_of_wind
      - 100m_v_component_of_wind
    expression: (_100m_u_component_of_wind**2 + _100m_v_component_of_wind**2)
**0.5
  cmip5:
    name: 10m_wind_speed
    scale: 1.6  # average scaling from 10m to 100m, based on one test locatio
n (approximate!)
```

In ERA5, vector components of 100m wind speed are provided. Our indicator is therefore a composition of these two variables, defined by the `expression` field, which is evaluated as a python expression. Note that variables that start with a digit are not licit in python and must be prefixed with an underscore _ in the `expression` field (only there).

For complex expressions, it is possible to provide a `mapping` field to store intermediate variables, for readability. This is used for the `relative_humidity` indicator:

```
- name: relative_humidity
  units: '%'
  era5:
    compose:
```

```
      - 2m_temperature
      - 2m_dewpoint_temperature
    expression: 100*(exp((17.625*TD)/(243.04+TD))/exp((17.625*T)/(243.04+T)))
    mapping: {T: _2m_temperature - 273.15, TD: _2m_dewpoint_temperature - 273
.15}
  cmip5:
    name: near_surface_relative_humidity
```

where `T` and `TD` are provided as intermediary variables, to be used in `expression`.

ERA5-hourly dataset can be retrieved via `frequency: hourly` field, and subsequently aggregated to monthly indicators thanks to pre-defined functions `daily_max`, `daily_min`, `daily_mean`, `monthly_mean`, `yearly_mean`. For instance:

```
- name: maximum_daily_temperature
  units: degrees Celsius
  offset: -273.15
  cmip5:
    name: maximum_2m_temperature_in_the_last_24_hours
  era5:
    name: 2m_temperature
    frequency: hourly
    transform:
      - daily_max
      - monthly_mean
```

This variable is available directly for CMIP5, but not in ERA5. It is calculated from `2m_temperature` from ERA5 `hourly` dataset, and subsequently aggregated. Note the ERA5-hourly dataset takes significantly longer to retrieve than ERA5 monthly. Consider using in combination with `--year 2000` to retrieve a single year of the ERA5 dataset.

Currently CMIP5 daily is not supported.

Netcdf to csv conversion

Convert netcdf time series files downloaded from the CDS Toolbox pages into csv files (note: this does not work for netcdf files downloaded via the cds api):

```
python netcdf_to_csv.py data/*nc
```

Help:
```
python netcdf_to_csv.py --help
```

Copernicus Climate Change Service